Quercetin hinders microglial activation to alleviate neurotoxicity via the interplay between NLRP3 inflammasome and mitophagy

Xiaojuan Han [a,b,c,1], Tianshu Xu [b,1], Qijun Fang [b], Huajun Zhang [b], Lijun Yue [b], Gang Hu [d,*], Lingyun Sun [a,c,**]

[a] Department of Rheumatology and Immunology, Department of Traditional Chinese Medicine, Nanjing Drum Tower Hospital Clinical College of Traditional Chinese and Western Medicine, Nanjing University of Chinese Medicine, Nanjing, China
[b] Department of Traditional Chinese Medicine, Nanjing Drum Tower Hospital, the Affiliated Hospital of Nanjing University Medical School, Nanjing, China
[c] Department of Rheumatology and Immunology, Nanjing Drum Tower Hospital, The Affiliated Hospital of Nanjing University Medical School, Nanjing, China
[d] Department of Pharmacology, Nanjing University of Chinese Medicine, Nanjing, Jiangsu, China

ARTICLE INFO

ABSTRACT

Activated microglia are an important type of innate immune cell in the brain, and they secrete inflammatory cytokines into the extracellular milieu, exert neurotoxicity to surrounding neurons and are involved in the pathogenesis of many brain disorders. Quercetin (Qu), a natural flavonoid, is known to have anti-inflammatory and antioxidant properties. Previous studies have shown that both increased reactive oxygen species (ROS) stress and decreased autophagy participate in the activation of microglial. In the current study, we showed that Qu significantly attenuated LPS-induced inflammatory factor production, cell proliferation and NF-κB activation of microglia. Importantly, Qu decreased the levels of NLR family, pyrin domain containing three (NLRP3) inflammasome and pyroptosis-related proteins, including NLRP3, active caspase-1, GSDMD N-terminus and cleaved IL-1β. Further study indicated that this anti-inflammatory effect of Qu was associated with mitophagy regulation. Importantly, Qu promoted mitophagy to enhance damaged mitochondrial elimination, which then reduced mtROS accumulation and alleviated NLRP3 inflammasome activation. Then, we confirmed that Qu treatment protected primary neurons against LPS-induced microglial toxicity and alleviated neurodegeneration in both depression and PD mouse models. Further IL-1β administration blunted these neuroprotective effects of Qu *in vitro* and *in vivo*. This work illustrated that Qu prevents neuronal injury via inhibition of mtROS-mediated NLRP3 inflammasome activation in microglia through promoting mitophagy, which provides a potential novel therapeutic strategy for neuroinflammation-related diseases.

1. Introduction

Recent studies have revealed that glial cells, important cellular components in addition to neurons in the central nervous system (CNS), play a more active role than previous considered [1,2]. Among all kinds of glial cells, microglia are resident immune surveillance cells of the CNS and have attracted much research owing to their diverse biological activities [3]. Physiologically, microglia assist in CNS synaptogenesis and brain homeostasis maintenance. In the case of neural damage, microglia play an important role in host defense and tissue repair by changing the phenotype and secreting many mediators [4]. However, when inappropriately or persistently activated, microglia secrete various inflammatory cytokines, such as interleukin 1β (IL-1β), into the extracellular milieu and participate in reactive oxygen species (ROS) generation, eventually damaging surrounding neuronal cells, which orchestrate microglia as neurotoxic mediators [4,5]. Accordingly, an increasing number of studies have suggested that activated microglia-mediated inflammation plays a vital role in the pathogenesis of many neurological and neurodegenerative diseases, such as brain ischemia, Alzheimer's disease (AD), major depressive disorder (MDD) and Parkinson's disease (PD) [6].

Abbreviations

PD	Parkinson's disease
MDD	major depressive disorder
NDDs	neurodegenerative diseases
IL-1β	interleukin 1 beta
LPS	lipopolysaccharides
CNS	central nervous system
ROS	reactive oxygen species
Qu	quercetin
i.p.	intraperitoneally
b.w.	body weight
SNpc	substantia nigra pars compacta
FST	forced swim test
TST	tail suspension test
IHC	immunohistochemical
PFA	paraformaldehyde

BSA	bull serum albumin
DAB	3,3′ -diaminobenzidine-tetrahydrochloride-dihydrate
IBA-1	ionized calcium binding adaptor molecule 1
Ly	lysate
SN	supernatant
CM	conditioned media
DAMPs	danger- or damage-associated molecular patterns
TH	tyrosine hydroxylase
LC3	microtubule-associated protein light chain 3
NLRP3	NLR family, pyrin domain containing protein 3
mtROS	mitochondrial reactive oxygen species
Mito Q	mitoquinone mesylate
3-MA	3-methyladenine;
DHE	dihydroethidium
MCM	microglia-conditioned media
Eth-D2	ethidium homodimer-2
GAPDH	glyceraldehyde-3-phosphate dehydrogenase

The above statements collectively demonstrate that inflammation represents the key regulator in various neurodegenerative disorders and highlight that microglia may be an important target for treating these inflammatory-related diseases. However, despite extensive efforts, many chemicals that target inflammation, such as caspase-1 inhibitors and IL-1β neutralizing antibody, have failed to induce the predicted clinical benefits in recent high-profile clinical trials [7]. Thus, further understanding of the detailed mechanisms of microglial activation, especially the interplay between inflammation and ROS, is needed to identify potential more effective therapeutic targets.

Among the various inflammatory cytokines, IL-1β produced by nod-like receptor (NLR) protein inflammasomes in microglia impairs motor and sensory neurons and is involved in many disorders [8,9]. The inflammasome serves as the main platform for caspase-1 activation and proinflammatory cytokine IL-1β maturation, and it is a multimeric protein complex that senses 'danger- or damage-associated molecular patterns (DAMPs) and responses to highly diverse stimuli [10]. Among the NLR family members, the NLRP3 inflammasome is the most highly expressed member in microglia and is most extensively studied [11]. Excessive NLRP3 inflammasome activation is involved in the pathogenesis of many brain disorders, including trauma, ischemia and major depressive disorder (MDD), as well as in NDDs such as PD [12]. Our previous study also demonstrated that increased NLRP3 activation in microglia participates in dopaminergic neuron death in PD mice [9].

In addition to the maturation of IL-1β, NLRP3 activation confers the release of IL-1β via pyroptosis, a newly discovered caspase-1-dependent programmed cell death process [13], occurs in multiple tissues, including brain [14,15]. In mice, pyroptosis acts downstream of the NLRP3 inflammasome, which transforms procaspase-1 into cleaved caspase-1 and then cleaves gasdermin (GSDM) family proteins, mostly GSDMD, to generate GSDMD N-termini and then form pores on the plasma membrane for IL-1β release [13,16]. Recent studies have revealed that excessive activation of pyroptosis leads to widespread cell death, causing tissue damage and plays an important role in infectious diseases [17]. With regard to CNS pathology, absent in melanoma 2 (AIM2) inflammasome-induced pyroptosis has been reported to be present in neurons and involved in traumatic brain injury (TBI) [14]. However, the importance of pyroptosis in brain injury, especially in brain immune cells, microglia, has not been fully studied.

Activation of NLRP3 inflammasomes requires two signaling pathways [18] as follows: Signal 1, the priming step, which was initially considered as the NF-κB-mediated upregulation of NLRP and pro-IL-1β; and signal 2, a direct inflammasome activator, which is needed to promote assembly of the NLRP3:ASC:pro-caspase-1 complex. Many molecules have been identified as activators of the second signal, including extracellular ATP, excess glucose, amyloids, urate and cholesterol crystals, contributing to a variety of diseases [19]. Recent studies have revealed that mitochondrial damage-associated signals, such as mtDNA and reactive oxygen species (mtROS), as well as cytosolic presentation of cardiolipin can promote NLRP3:ASC:pro-caspase-1 complex assembly [20]. More interestingly, subsequent studies have indicated that extracellular ATP-induced activation of the NLRP3 inflammasome leads to NLRP3-dependent dissipation of the mitochondrial membrane potential [21,22], generating more mitochondria signals that then amplify inflammasome assembly and activation [20,23]. Interestingly, promoting autophagy, a quality control process, has been proposed to negatively regulate NLRP3 inflammasome activation [24,25]. The above findings suggest that inflammasome activation may be promoted by signals associated with damaged mitochondria, which can be degraded in lysosomes through mitophagy [23,26]. The role of mitochondrial damage in the activation of NLRP3 inflammasome encourages us to speculate that promotion of the autophagic elimination of damaged mitochondria may inhibit the overactivation of NLRP3 inflammation in microglia and suggests that a mitophagy promotion and inflammation inhibition based dual-targeted therapeutic strategy may be a better choice than any single-targeted strategy.

Recently, considerable attention has been focused on identifying naturally occurring substrates, especially natural phytochemicals, owing to the wide range of biological activities [27]. Flavonoids are natural polyphenolic compounds that have largely attracted the attention of the scientific community and may be promising therapeutics for many disorders [27]. Quercetin (3,3',4',5,7-pentahydroxyflavone; Qu), one of the most common plant flavonoids and prominent dietary antioxidants in the human diet [28], exists in various traditional Chinese herbal medicines, tea, fruit and other vegetables, and it has been approved in clinical trials [29]. Qu has been proposed to conserve antifibrotic, antiviral, anticancer, anti-inflammatory and antioxidative properties [27]. A previous study has also demonstrated that Qu promotes autophagic progression by inducing the appearance of autophagic vacuoles, conversion of LC3-I to LC3-II and activation of autophagy genes [30].

Because Qu has been used as a healthy supplement for years and conserves antioxidative, anti-inflammatory and autophagy-promoting effects, we hypothesized that Qu may be a promising and multi-targeting inhibitor of microglial activation, thereby protecting neurons from microglia-/inflammation-mediated toxicity. The aim of this study was to investigate whether Qu exerts neuroprotective effects by inhibiting microglial activation and to demonstrate the underlying mechanism.

2. Materials and methods

2.1. Chemicals and reagents

LPS (L3023), penicillin-streptomycin (V900929), pentobarbital sodium (Y0002194), and 3-MA (M − 9281) were purchased from Sigma-Aldrich (St. Louis, MO, USA). Quercetin (117-39-5) for *in vivo* treatment was purchased from Nanjing Jingzhu Bio-technology Co.,Ltd (Nanjing, China), quercetin (HPLC > 99.0%, S2391) for *in vitro* experiments were obtained from Selleck.cn (Houston, TX, USA). Mito Q (S8978) was obtained from Selleck.cn (Houston, TX, USA). MitoSOX™ Red Mitochondrial Superoxide Indicator (M36008), dihydroethidium (DHE; D23107), YO-Pro-1 iodide (491/509) (Y3603), Ethidium Homodimer-2 (EthD-2; E3599) and FluoSpheres™ carboxylate-modified microspheres (F8825) were purchased from Thermo Fisher Scientific (Rockford, USA). IL-1β (401-ML/CF) was purchased from R&D Systems (Minneapolis, MN, USA). ELISA kits for murine IL-1β (EM004-96) was purchased from ExCell Bio (Taicang, China). For animal experiments, Qu was dissolved in a solution of 2% DMSO +30% PEG300 + 2% Tween 80 in sterile ddH$_2$O. The solution without Qu was used as vehicle. For cell experiments, Qu was prepared in DMSO (Sigma) and PBS (final DMSO concentration is 0.01%), pH 7.4.

For western blotting analysis, the following antibodies were used: anti-p-IKKβ Ab (1:1000, Cell Signaling Technology, 2697); anti-IKKβ Ab (1:1000, Cell Signaling Technology, 8943); anti-iNOS Ab (1:1000, Abcam, ab49999); anti-Nrf2 Ab (1:1000, Cell Signaling Technology, 33649); anti-p65 Ab (1:1000, Cell Signaling Technology, 8242s); anti-caspase-1 Ab (1:500, Millipore, 06-503-1); anti-caspase-1(p20) Ab (1:500, AdipoGen, AG-20B-0042); anti-NLRP3 Ab (1:1000, AdipoGen, AG-20B-0014-C100); anti-IL-1β Ab (1:500, Sigma, AB10626); anti-GSDMD Ab (1:1000, Sigma, G7422) ; anti-p62 Ab (1:1000, Cell Signaling Technology, 5114); anti-LC3 Ab (1:1000, Cell Signaling Technology, 2775); anti-PINK1 Ab (1:1000, Abcam, ab23707); anti-Parkin Ab (1:1000, Abcam, ab15954); anti-TH Ab (1:1,000; Abcam, ab6211); anti-β-actin Ab (1:2000, Proteintech, 20536-1-AP); horseradish peroxidase-conjugated goat anti-mouse or rabbit IgG secondary antibody (1:2,000; Thermo, 31430 and 31460).

For immunohistochemical or immunofluorescence staining analysis, the following antibodies were used: anti-IBA1 Ab (1:500, Wako, 019–1974); anti-TH Ab (1:800, Sigma, T1299); anti-CD68 Ab (1:800, Proteintech, 66231-2-Ig); anti-NLRP3 Ab (AdipoGen, AG-20B-0014-C100; 1:500); anti-p62 Ab (1:1000, Cell Signaling Technology, 5114); anti-Tomm20 Ab (1:800, Proteintech, 11802-1-AP); anti-MAP2 Ab (1:1000, Proteintech, 17490-1-AP); Alexa Fluor 488-conjugated donkey anti-mouse IgG (1:1000, Invitrogen, A21202); Alexa Fluor 488-conjugated goat anti-rabbit (1:1000, Invitrogen, A11008); Alexa Fluor 555-conjugated goat anti-rabbit IgG (1:1000, Invitrogen, 21,432); Alexa Fluor 555 goat anti-mouse IgG (1:1000, Invitrogen, 21,422).

2.2. Cells cultures and treatments

Primary microglia were obtained from postnatal (P1 to P2) mice and conducted as described previously [9]. Briefly, whole brains were removed, dissected and then mechanically dissociated to remove the membranes and large blood vessels. Next, the dissected brains were digested with trypsin-EDTA and then filtered through a 100-μm filter to obtain a single cell suspension. Subsequently, the cells were plated on poly-L-lysine-precoated cell culture flasks containing Dulbecco's modified Eagle's medium (DMEM) supplemented with FBS (10% v:v) and penicillin/streptomycin (1% v:v). After 7–10 days, the microglia were dissociated by shaking the flasks several times, harvested by centrifugation (300 g × 10 min) and then plated on poly-L-lysine-precoated 24-/96-well plates at × 10^5 cells/ml in complete cell culture medium for subsequent use.

Primary neuron cultures were conducted as described previously [31]. In brief, the hippocampus and mesencephalic tissues of C57BL/6

mice on embryonic day 14/15 (E14/15) was carefully removed, mechanically dissociated to remove the membranes and large blood vessels and then dissected. Next, they were digested with trypsin-EDTA (Cat 25200056, Gibco™, Thermo Fisher Scientific, Rockford, USA) and then filtered through a 100-μm filter to obtain a single cell suspension. Subsequently, the cells were plated on poly-L-lysine-precoated 12-/24-well plates at 2.5 × 10^5 cells/ml containing Neurobasal medium (Cat 21103049, Gibco™) supplemented with B27 (2% v:v, Cat 17504044, Gibco™) and penicillin/streptomycin (0.5% v:v). The culture medium was changed every 3 days and cells can be used at 7–10 days. Both hippocampus and mesencephalic primary neurons were treated with microglia-conditioned media (MCM) mixed with the neurobasal culture medium (1:2) for 12 h.

Cell lines: the authenticated mouse microglia BV2 cell line were cultured in 10% FBS and 1% penicillin/streptomycin at 37 °C in a 5% CO$_2$ atmosphere and used at passages 4 to 14. In the experiments, BV2 cells were treated with LPS (100 ng/ml) or different doses of Qu for 24 h. Ka (30, 60 μM, 1 h) primed-BV2 cells were stimulated with LPS (100 ng/ml) for 24 h and ATP (5 mM) for 30 min. Qu (30 μM, 1 h) with (or without) 3-MA (5 mM, 1 h) primed-BV2 cells were stimulated with LPS (100 ng/ml) for 24 h.

2.3. Immunocytochemistry and confocal microscopy

Primary microglia and BV2 cells were seeded at 1 × 10^5 cells per well in 12 well glass slides, and rested overnight for proper attachment. Then, the cells were treated as designed. After the treatment, the cells were washed twice with PBS and fixed with 4% PFA, permeabilized with 0.01% Triton X-100 and blocked in 5% BSA. The cells were then incubated overnight with primary antibodies. Secondary fluorescent antibodies were added for 1 h and DAPI was used for nuclear counterstaining. Samples were then imaged by fluorescence microscopy (Olympus, Tokyo, Japan).

2.4. Cell viability CCK-8 assay

The changed cell viability of Qu treatment was detected by cell counting kit-8 (CCK-8 Kit, c0037, Beyotime, Shanghai, China). In brief, BV2 cells were seeded in a 96-well plate and then treated with different concentrations of Ka (3, 10, 30, 100, 300 μM) or plus LPS (100 ng/ml) for 24 h or 48 h. Then 10 μl of CCK-8 reagent was added to each well for 4 h. Finally, the absorbance was detected by the Multiskan Spectrum (Thermo Fisher Scientific) at 450 nm.

2.5. Western blotting analysis

In vitro experiment, BV2 cells were mainly used and prepared for the western blotting analysis because they are more easily acquired and repeatable than primary microglia. Cells or brain tissues were lysed in the RIPA buffer (50 mM Tris (pH 7.4), 150 mM NaCl, 1% NP-40, 0.5% sodium deoxycholate, 0.1% SDS supplemented with protease and phosphatase inhibitors. Protein concentrations were determined with the Micro BCA Kit (Beyotime, Shanghai, China). A 30-μg protein of each sample were separated by SDS-PAGE using polyacrylamide TGX gels (Bio-Rad) and then transferred to polyvinylidene difluoride (PVDF) membranes (Millipore, Bedford, MA). After blocking, PVDF membranes were incubated with various specific primary antibodies in TBST at 4 °C overnight then washed and incubated in corresponding horseradish peroxidase (HRP) conjugated secondary antibodies for 1 h at room temperature. Immunoreactive bands were visualized and detected by enhanced chemiluminescence (ECL) and analyzed using the Image-Quant™ LAS 4000 imaging system (GE Healthcare, Pittsburgh, PA, USA).

2.6. Purification of cell culture supernatant (SN) protein

The cell culture SN protein analysis experiments were carried out as described previously [9]. Briefly, the cell culture SN was collected and centrifuged to remove the dead cells. Then, 500 µl of SN was transferred into new tubes, 500 µl of methanol and 125 µl of chloroform were added, and centrifuged at 21,000 g for 5 min to precipitate the SN proteins. The upper phase was discarded without touching the protein layer, another 500 µl of methanol was added and then the mixture was centrifuged at 21,000 g for 5 min, then the pellet was dried at 37 °C for 5 min. Ultimately, 30 µl of 2 × loading buffer was added and vortexed. The samples were boiled and loaded onto 12–15% gels for western blotting analysis.

2.7. Reverse transcription (RT)-and real time quantitative (q) PCR

Total RNA was extracted from brain tissues and cultured cells using Trizol reagent (15596026, Invitrogen, Carlsbad, CA, USA). Reverse transcription was carried out using TAKARA PrimeScript RT reagent kit (RR036A, TaKaRa, Japan). Realtime qPCR was carried out using SYBR Green Master Mix (04913914001, Roche) in a StepOnePlus instrument (Applied Biosystems). The primers were purchased and validated from Generay (Shanghai, China). The primers used for qPCR were shown in Supplementary Table 1.

2.8. Intracellular and mitochondrial ROS detection

Intracellular ROS was measured using dihydroethidium (DHE) as described previously [32]. Cells pretreated with (or without) Qu were primed with LPS (100 ng/ml, 24 h). The cells were then incubated with 2 µM DHE for 30 min at 37 °C and washed twice with PBS, followed by staining with Hoechst 33342 to indicate nucleuses for 10 min. Mitochondrial ROS were measured using MitoSOX as described [20]. Briefly, BV2 cells, pretreated with (or without) Qu (30 µM, 1 h) and 3-MA (5 mM, 1 h), were primed with LPS (100 ng/ml, 24 h) followed by treatment with ATP for 30 min. Then the cells were washed with PBS and loaded with 4 µM of MitoSOX for 20 min and washed twice with PBS. Fluorescence intensity was observed and photographs were captured by fluorescence microscopy (Olympus, Tokyo, Japan).

2.9. Hoechst staining

To quantify apoptotic cells, monolayer BV2 cells or primary neurons were fixed and stained with Hoechst 33,324 (Sigma, St Louis, MO, USA) (1 µl diluted in 500 µl PBS) for 10 min as described previously [33]. The morphological features of apoptosis (high-density fluorescence with nuclear shrinkage, chromatin fragmentation, and condensation) were observed and monitored by fluorescence microscopy (Olympus, Tokyo, Japan).

2.10. TH immunoreactivity neurite length measurement

To quantify the TH immunoreactivity neuronal processes, primary mesencephalic neurons were fixed and followed by immunocytochemistry as described above. Thirty TH immunoreactivity (TH-ir) neurons were randomly selected and captured by a Nikon Optical TE2000-S inverted microscope (Nikon, Melville, New York). The length of each TH-ir cell neurite was traced from the perinuclear region to the end of the neurite using the measurement function of Image J (NIH software). The values were normalized to that obtained from control culture.

2.11. Microglia phagocytosis assay

Primary microglia were seeded in a 12-well plate glass slides as described [9]. The cells were then pretreated with Qu and stimulated with LPS for 24 h. To assess microglial phagocytotic activity, 0.5 µl/ml latex beads (2-µm, Invitrogen) were added into each well as described

[34]. After 2 h, the cells were washed with PBS and fixed with 4% PFA for 10 min at room temperature then rinsed with PBS and observed by fluorescence microscopy (Olympus, Tokyo, Japan).

2.12. Enzyme-linked immunosorbent assay

Cultured cell supernatant samples were collected after stimuli. The concentration of IL-1β in cell culture supernatants was measured by mouse IL-1β ELISA kits (ExCell Bio, EM004-96) according to the manufacturer's instructions.

2.13. Dye uptake

Dye uptake assay was conducted as described [14]. BV2 cells were pretreated with Qu for 1 h and stimulated with LPS plus ATP for 24 h. Triton X-100 detergent (0.1%) was used as a positive control. Both YO-PRO-1 iodide (0.2 mM) and ethidium homodimer-2 (Eth-D2) (2 mM) were added for 15 min. Cells were then stained with Hoechst 33342 and images were captured using an inverted microscope (Olympus, Tokyo, Japan).

2.14. Experimental animals

C57BL/6J mice (male, 3-month old) were obtained from Nanjing Medical University Animal Core (Nanjing, China). Mice were maintained and bred in the animal facility at Nanjing Drum Tower Hospital. All animals were maintained with free access to pellet food and water under specific pathogen-free conditions. Animal welfare and experimental procedures were performed in accordance with the Guide for the Care and Use of Laboratory Animals (National Institutes of Health, the United States).

2.15. Stereotaxic surgery, induction and treatment of LPS- induced PD and depression mouse model

For LPS-induced PD mouse model induction, stereotaxic surgery under pentobarbital sodium anesthesia (40 mg/kg b.w., i.p.) was performed as described [9]. The SNpc of 3-month-old C57BL/6 mice were microinjected bilaterally with LPS (0.5 µg in 1 µl of saline, 0.2 µl/min) using the following coordinates relative to the bregma: A/P −3.0 mm, R/L ± 1.3 mm, and D/V −4.5 mm, which can induce the typical pathologic changes of PD. The respective controls were injected with equivalent volumes of saline. For LPS-induced depression mouse model induction, mice were intraperitoneally injected with LPS (1 mg/kg b.w.) or saline as control for 5 successive days as described [35]. Such regimen can induce depression-like behavioral changes in mice and is widely used.

To evaluate the protection of Qu in the PD and depression model of LPS-toxicity, mice were randomly divided into the following groups: saline-treated group, LPS + vehicle-treated group, LPS + Qu (30 mg/kg b.w., i.p., daily)-treated group, LPS + Qu (60 mg/kg b.w., i.p., daily)-treated group, and LPS + Qu (60 mg/kg b.w., i.p., daily) + IL-1β (15 µg/kg b.w., i.p., daily)-treated group. For the pharmacological evaluation, mice received Qu treatment 3 d prior to treatment with LPS and over the 5 LPS injection days in depression model and 3 d prior to injection with LPS and 7 d afterwards in PD model. For IL-1β treatment, mice were given recombinant IL-1β (15 µg/kg b.w., i.p., daily) injection for two days followed the last injection of Qu. Control mice received saline only. All drugs were administered between 2:30 p.m. and 3:30 p. m. Doses of Qu were selected based on the preliminary animal [36,37] and human studies (with 30/60 mg/kg b.w. corresponding to a dose of 2.1/4.2 g for a 70 kg individual) without any adverse effects associated with Qu administration [29,38]. To evaluate the equilibrium and depressive performance, mice were subjected to behavioral testing blinded to groups. Finally, all mice were anesthetized and sacrificed for brain proteins detection and immunohistochemistry analysis.

2.16. Behavioral analysis

Two days after the final injection of Qu, the forced swim test (FST) and tail suspension test (TST) were performed as described before [35]. For the FST, mice were forced to swim individually in a cylinder (height, 25 cm; diameter, 15 cm) containing 15 cm water maintained at 22 ± 2 °C. Mice were judged to be immobile to keep their heads above water, which was characterized by motionless floating in the water with an upright position and only necessary slight movements. The duration of immobility was recorded during the last 4 min of the 6 min test by TailSuspScan (Clever Sys). For TST, mice were suspended in the apparatus box (50 × 50 × 50 cm) by wrapped mice tails with adhesive tape. Each test period lasted 6 min, with the first 2 min as the habituation period. During the last 4 min, duration of immobility (hanging passively and motionless) was recorded with TailSuspScan (Clever Sys). The rotarod test was performed as described in our previous work [39]. In brief, mice were acclimatized to the rotarod for 2 consecutive days then were tested at 20 rpm for 300 s for other 3 consecutive days. The latency to fall was recorded using Rotarod Analysis System (Jiliang, Shanghai, China).

2.17. Brain sample collection

At the end of the experiments, mice were anesthetized by sodium pentobarbital (40 mg/kg b.w., i.p.). For qPCR and western blotting analysis, the whole brains were rapidly extracted from animals then the midbrain or hippocampus samples were quickly dissected, pre-frozen by liquid nitrogen. All samples were stored at −80 °C until analysis.

For immunohistochemical (IHC) analysis, mice were perfused transcardially with 4% paraformaldehyde (PFA). Brains were extracted, post-fixed, dehydrated, embedded in OCT (Tissue-Tek), and serial sections of the brains were cryosectioned (30 μm per slicen) through each entire hippocampus and midbrain using a freezing microtome (Leica CM1950, Nussloch, Germany). All sections were collected in six separate series and brain slices were stored in 50% glycerin and frozen in −20 °C until analysis.

2.18. Histological analysis, IHC, and immunofluorescence

For IHC or immunofluorescence staining, the brain sections were prepared as described in our previous study [9]. Brain slices were rinsed in PBS (followed by 3% H_2O_2 for 10 min for IHC assay) then incubated with 0.3% Triton X-100 in PBS supplemented 5% Bull Serum Albumin (BSA) for 1 h. After that, slides were incubated with the primary antibodies in PBS containing 5% BSA at 4 °C overnight, then washed and incubated in secondary antibodies for 1 h at room temperature, followed by incubating with diaminobenzidine (DAB) or mounting in DAPI (Cat P36931, ThermoFisher scientific) as immunofluorescent staining for 5 min. The total numbers of TH-positive neurons in the SNpc and IBA-1-positive microglia in the hippocampus or cortex were obtained stereologically by using the optical fractionator method with Micro-BrightField Stereo-Investigator software (MicroBrightField, Williston, VT, USA).

2.19. Statistical analysis

Data were presented as mean ± SEM. The significance of difference was determined by Student's *t*-test or one-way analysis of variance (ANOVA) followed by Tukey's post hoc test. Difference was considered significant at $P < 0.05$.

3. Results

3.1. Effects of Qu on the survival and inflammatory factor expression of primary microglia and BV2 cells

First, to examine the effect of Qu on the survival of microglial cells, both the primary microglia and the murine microglial BV2 cells were treated with different concentrations of Qu for 24 h, and a CCK-8 assay was performed to determine its cytotoxicity. As shown, Qu treatment at concentrations of 100 μM or lower had no effect on the viability of BV2 cells (Fig. 1b) and primary microglia (Fig. S1a) compared with untreated controls. To evaluate the anti-inflammatory effects of Qu, LPS-stimulation was included. BV2 cells were pretreated with Qu for 1 h followed by LPS (100 ng/ml) treatment for 24 h. Treatment with LPS alone or plus Qu (30 and 100 μM, safe concentrations) developed no significant changes in the survival ratio of cells (Fig. 1c). A Hoechst staining assay was then performed, which shows high-density fluorescence with chromatic agglutination and karyopyknosis to indicate compromised or apoptotic cells. Consistently, under a fluorescence microscope, Qu had no effect on chromatin condensation or nuclear shrinkage in LPS-treated BV2 cells (Fig. 1d). Further functional studies showed that LPS exposure increased the mRNA levels of Il-1β, Il-6 and Tnfα. These pro-inflammatory mediators were significantly inhibited by Qu in both BV2 cells (Fig. 1e–g) and primary microglia (Figs. S1b–d). Since Qu induced significant inhibitory effects at 30 μM and 60 μM concentration in a concentration-dependent manner, we observed these concentrations in the subsequent studies. These results indicate that Qu inhibits inflammatory activation without affecting the viability of microglial BV2 cells.

3.2. Qu inhibits LPS-induced proliferation of primary microglia and reduces LPS-induced microglial phagocytosis

In addition to the upregulation of inflammatory factors, enhanced proliferation is another hallmark of microglial activation, leading to an increase in cell density that further amplifies the inflammatory response [6]. We then investigated the effect of Qu on LPS-induced microglial proliferation. As shown in Fig. 2a and b, LPS treatment resulted in a significant increase in the proliferation of primary microglia, which was attenuated by Qu pretreatment in a dose dependent manner.

Since active microglia develop enhanced phagocytosis, we further investigated whether the inhibitory effect of Qu on microglial activation was associated with decreased phagocytic activity. To test this hypothesis, the phagocytosis activity was measured by a phagocytosis assay using fluorescence microspheres. As shown in Fig. 2c and d, LPS treatment significantly increased the microsphere phagocytosis in microglia (−11.3-fold). Qu at 30 and 60 μM concentrations dramatically attenuated the phagocytosis induced by LPS stimulation (Fig. 2c and d). In addition, increased phagocytic activity displays a high level of CD68, a lysosomal-localized indicator [40]. For conformation, the expression of CD68 in microglia was measured by costaining with CD68 and microglial marker, IBA-1. The results revealed that exposure to LPS caused a significant increase in intracellular CD68 fluorescence intensity, which was significantly suppressed by pretreatment with Qu (Fig. 2e and f). These results collectively suggest that Qu plays a crucial role in the regulation of the microglial proliferation and phagocytotic activity.

3.3. Qu suppresses LPS-induced intracellular ROS production and NF-kB (p65) activation in BV2 cells

Increased intracellular ROS production is another marker of microglial activation, which in turn activates microglia to secrete more proinflammatory factors and exacerbate inflammation [41]. To determine whether Qu attenuates LPS-induced ROS production, DHE assays were performed to detect intracellular ROS. The results showed that exposure of microglia to LPS for 24 h caused a significant increase in
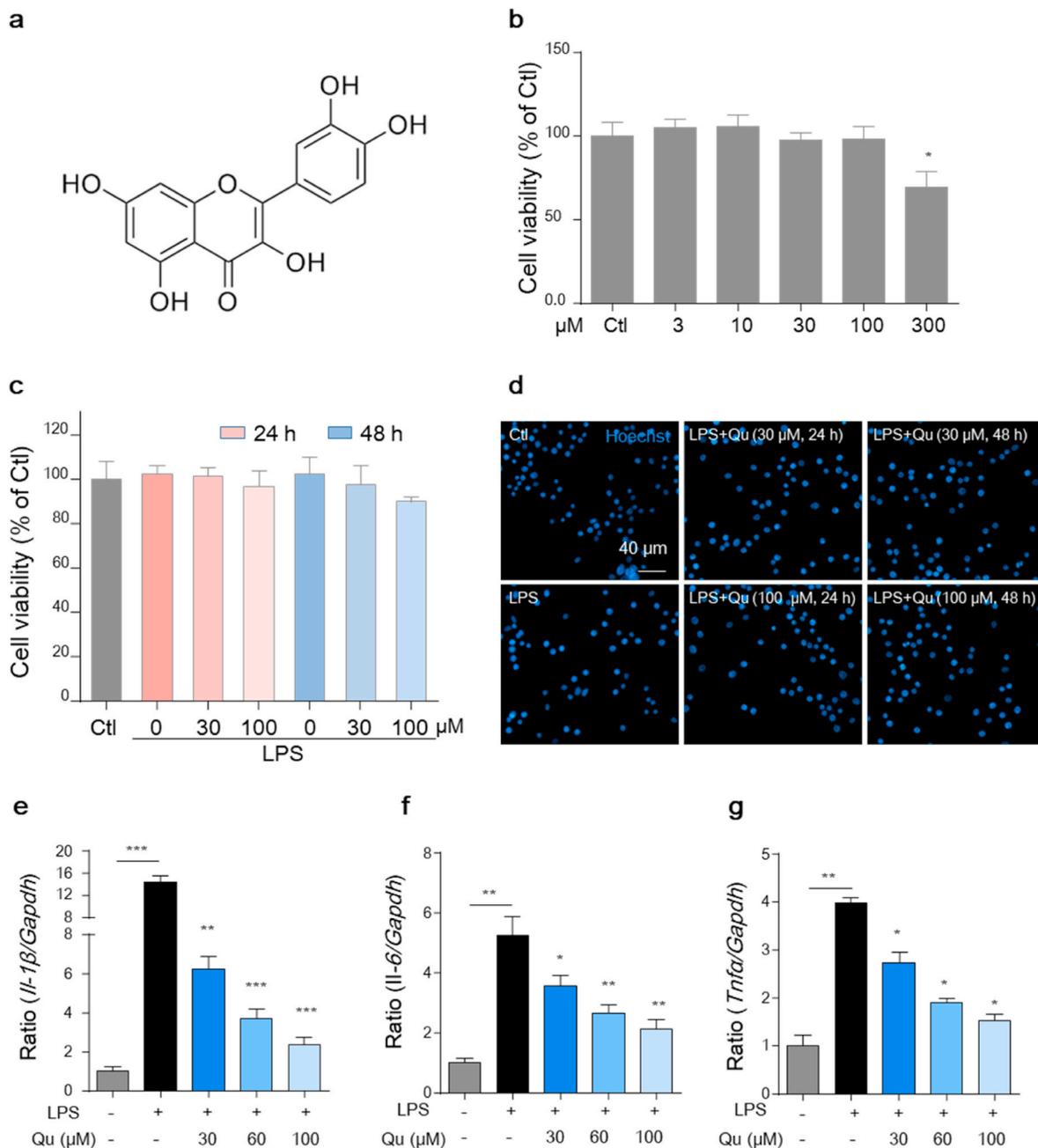
Fig. 1. Qu suppresses the inflammatory activation in microglial BV2 cells.
(a) The chemical structure of quercetin. (b) BV2 cells were treated with Qu (0–300 μM, 24 h), and then the CCK-8 assay was performed to determine cell viability. (c–d) Cells were treated with Qu (0–100 μM) for 1 h followed by LPS (100 ng/ml) exposure for 24 or 48 h. Cell viability was assessed by the CCK-8 assay (c) and Hoechst staining (d). Scale bar, 40 μm. (e–g) Effects of LPS and Qu on the expression of IL-1β (e), IL-6 (f) and Tnfα (g) in BV2 cells as analyzed by qPCR (normalized to the control group). Data are shown as the e ± SEM and are representative of at least three independent experiments. ns, not significant,*$P < 0.05$, **$P < 0.01$ and ***$P < 0.001$ by one-way ANOVA followed by Tukey's post hoc test. Ctl, untreated control; Qu, quercetin; LPS, lipopolysaccharide.

DHE-positive cells (Fig. 3a and b). However, pretreatment with Qu markedly suppressed LPS-induced ROS production in microglia (Fig. 3a and b). Besides, the markedly induced expression of iNOS, which mediates the synthesis of large amounts of NO, was also confirmed by western blot analysis. Qu inhibited LPS-induced iNOS expression at the protein level (Fig. 3c–e). Further Nrf2 signaling, which regulates the expression of antioxidant enzymes, was analyzed. And we found that the LPS-induced reduction of Nrf2 within the nucleus was significantly revised or even enhanced in Qu-treated cells (Fig. 3d, f).

Given that activated NF-κB subunit plays an important role in mediating the expression of pro-inflammatory cytokines and the generation of ROS, we further examined the effect of Qu on the activation of

NF-κB in BV2 cells using western blot analysis. LPS treatment induced dramatic NF-κB activation compared with the control, as indicated by a significant increase of IKKβ phosphorylation (Fig. 3c, g) and increased p65 subunit translocation into the nucleus (Fig. 3d, h), which was distinctly attenuated by Qu treatment (Fig. 3c–d, g-h). These results demonstrate that Qu reduces microglial activation-related intracellular ROS generation and indicate that the anti-inflammatory effect of Qu in microglia is associated with the suppression of NF-κB activity.
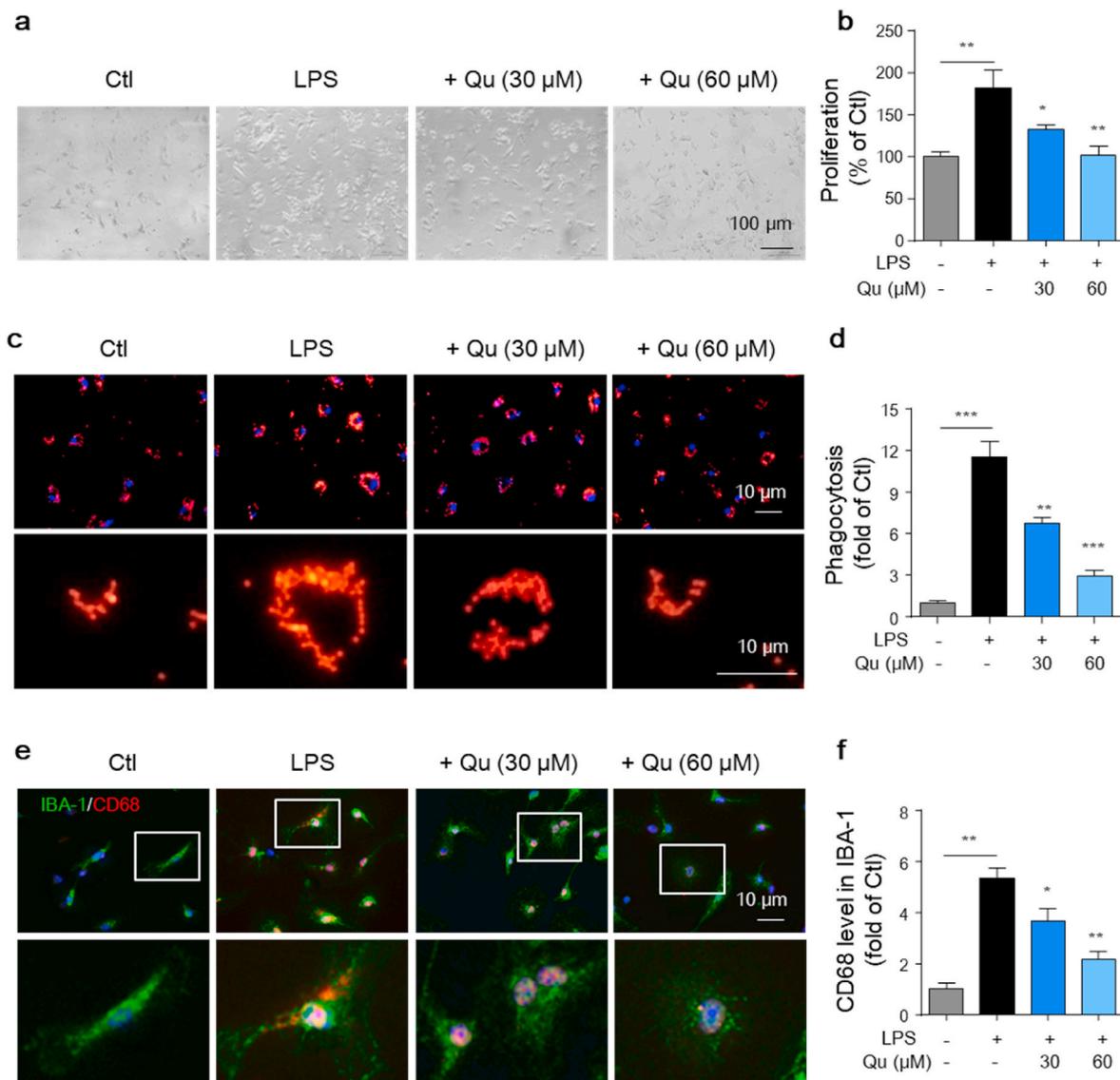
Fig. 2. Qu inhibits LPS-induced proliferation and phagocytotic activity in microglia. Primary microglia were treated with 30 and 60 μM Qu for 1 h, followed by LPS (100 ng/ml) treatment for 24 h (a–b) Effects of Qu on LPS-induced proliferation changes in primary microglia observed by phase-contrast microscopy, and cell numbers were quantified (normalized to the control group). Scale bar, 100 μm. (c–d) Phagocytosed microspheres were imaged by fluorescence microscopy (c). Scale bars, 10 μm. The density of beads was analyzed and quantified (d) (normalized to the control group). (e–f) Phagocytotic activity was assessed by immunostaining CD68 (lysosomal phagocytic degradation marker) in IBA-1$^+$ microglia and observed by fluorescence microscopy (e). Scale bar, 10 μm. The mean fluorescence intensity (MFI) of CD68 was quantified (f) (normalized to the control group). Values are shown as the mean ± SEM of at least three independent experiments. *$P < 0.05$ and **$P < 0.01$, ***$P < 0.001$ by one-way ANOVA followed by Tukey's post hoc test. Ctl, untreated control; Qu, quercetin; LPS, lipopolysaccharide.

3.4. Qu suppresses the activation of NLRP3 inflammasome and related pyroptosis in LPS and ATP -treated BV2 cells

NLRP3 inflammation activation is a key mediator of the increased inflammatory factors release in microglia and plays an important role in neurodegeneration [12]. To determine the effects of Qu on NLRP3 inflammasome activation, LPS-primed BV2 cells were pretreated with Qu followed by an ATP challenge, which acts as a second signal and is needed for the NLRP3 inflammasome assembly. Qu inhibited the LPS-induced increase in the expression of NLRP3 inflammation-related proteins, including NLRP3, NLRP3-dependent caspase-1 activation, and IL-1β maturation, in a concentration-dependent manner as evidenced by western blot analysis (Fig. 4a–c). The inhibitory effect of Qu on the maturation and release of IL-1β was further confirmed by ELISA (Fig. 4d).

NLRP3 inflammation activation also leads to the cleavage of full-length GSDMD to generate the GSDMD N-terminus as the effector molecule of pyroptosis [13]. We observed an increase in the level of the GSDMD N-terminus in LPS plus ATP-treated BV2 cells, which was significantly inhibited by Qu pretreatment (Fig. 4a, c). Activated GSDMD-N forms oligomeric pores in the plasma membrane and is required for cleaved IL-1β release to extracellular, which is a distinctive characteristic of pyrotosis [42]. The pores have an average inner diameter of approximately 13 nm, which allows only small molecules to pass through. Thus, the combined use of Eth-D2, a larger membrane impermeable dye, and YO-PRO-1 iodide, a small membrane impermeable dye, allows visualization of pyrotosis-related pores [14]. To investigate whether Qu-mediated NLRP3 inhibition also shares this feature, we applied these dyes to LPS plus ATP-treated BV2 cells. Triton 0.1% served as a positive control for dye uptake. We found that NLRP3 inflammasome stimulation resulted in an increased uptake of YO-PRO-1 iodide (green) with the exclusion of Eth-D2 (red), which was significantly inhibited by Qu pretreatment (Fig. 4 e-f). These results demonstrate that Qu inhibits NLRP3 inflammasome activation and
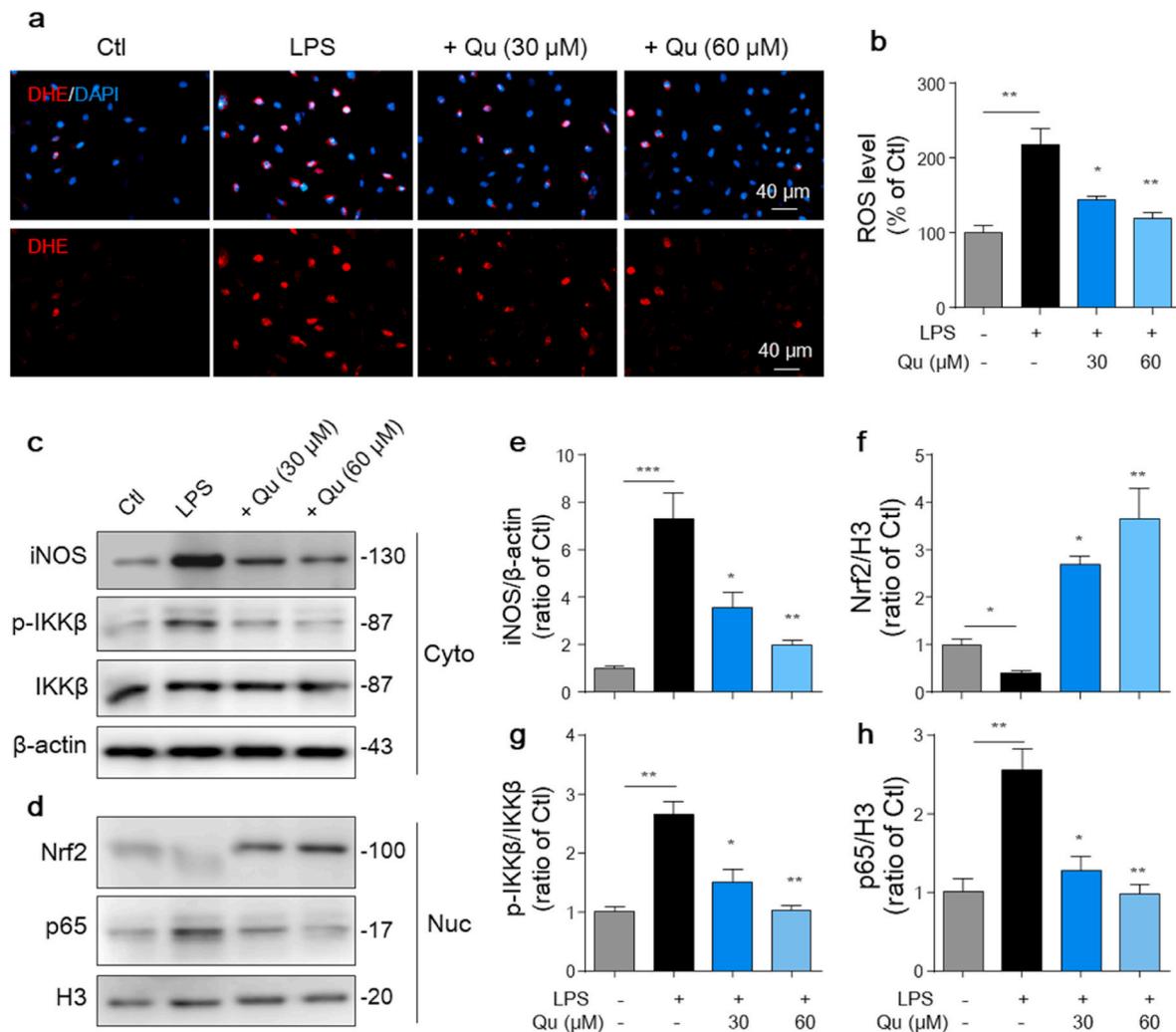
Fig. 3. Qu inhibits LPS-induced ROS generation, NF-κB (p65) activation and activates Nrf2 signaling in BV2 microglial cells. Primary microglia and BV2 cells were pretreated with Qu (30–60 μM) for 1 h followed by LPS (100 ng/ml) exposure for 24 h (a–b) Intracellular reactive oxygen species (ROS) accumulation was measured by the dihydroethidium (DHE) assay and monitored by fluorescence microscopy. Scale bars, 40 μm. (c–h) iNOS protein expression in BV2 cells was determined by Western blotting assay (c) and quantified by densitometry (e). Phosphorylation of IKKβ and nuclear (Nuc) translocation of NF-κB (p65) was determined by Western blot analysis (c–d) and quantified by densitometry (g–h). Nuclear accumulation of Nrf2 was determined by Western blot assay (d) and quantified by densitometry (f) (normalized to the control group). Data are shown as the mean ± SEM of at least three independent experiments. *$P < 0.05$, **$P < 0.01$ and ***$P < 0.001$ by one-way ANOVA followed by Tukey's post hoc test. Ctl, untreated control; Qu, quercetin; LPS, lipopolysaccharide; Nuc, nucleus; Cyto, cytoplasm.

NLRP3-mediated pyroptosis in microglial BV2 cells.

3.5. Qu promotes mitophagy and decreases mito-ROS production in LPS and ATP-stimulated BV2 cells

NLRP3 inflammasome agonists trigger mitochondrial damage [20, 22], which in turn functions as the second signal to promote NLRP3 inflammation activation [19] (Fig. 5a). Normally, damaged mitochondria are eliminated via mitophagy [43] and blunted mitophagy forms a feedback loop with NLRP3 inflammation to amplify the inflammatory response [22]. To investigate whether mitophagy is involved in the anti-inflammatory effect of Qu, we first examined the levels of autophagy-associated proteins. As shown in Fig. 5b–f, in cultured BV2 cells, the level of microtubule-associated protein light chain 3 (LC3)-II was remarkably lower, while the expression of p62, a substrate of autophagy, was markedly increased in both cytosal and mitochondrial protein extracts from LPS + ATP-treated cells, as measured by western blot, which was significantly reversed by Qu treatment (Fig. 5b–f). As a specialized form of autophagy, mitophagy is controlled by mitophagy-related proteins including PINK1, Parkin and BNIP3. We also

found that the expressions of Parkin and PINK1 were much lower in mitochondrial fraction of LPS + ATP treated BV2 cells (Fig. 5b, g-h). Qu treatment restored the mitochondrial level of Parkin and PINK1. We further tested the changes in mitophagy by coimmunostaining of p62 and Tomm20 (a protein located in the outer mitochondrial membrane) with bafilomycin added to prevent autophagosome fusion with lysosomes. LPS + ATP treatment induced more p62-containing aggregates colocalized with or adjacent to mitochondria, indicating blunted autophagic degradation of mitochondria, which was also reduced by Qu pretreatment (Fig. 5i and j).

Increased accumulation of damaged mitochondria exacerbates mitochondrial oxidative stress and enhances mtROS production [20]. Additionally, Qu significantly reduced the robust ROS-generating mitochondria, as determined by MitoSOX staining (Fig. 5k-l), which was comparable to the addition of Mito Q, a mitochondrial-specific antioxidant. These results support that damaged mitochondria in LPS + ATP-treated BV2 cells are mobilized by mitophagy for removal and that Qu promotes mitophagy to reduce mtROS accumulation.
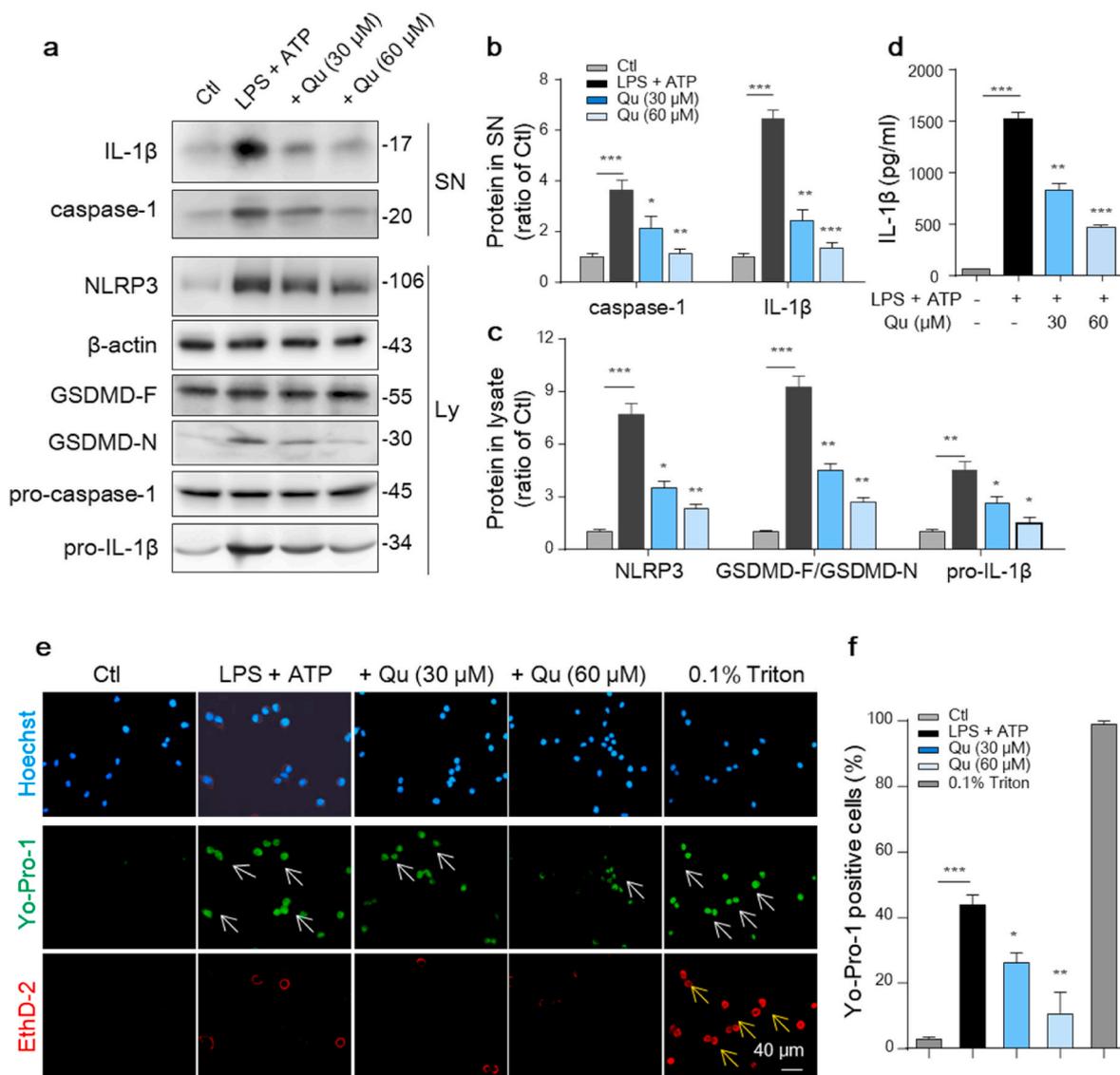
Fig. 4. Qu inhibits the LPS-induced NLRP3 inflammasome and related pyroptosis in BV2 cells. Qu (30 and 60 µM, 1 h)-pretreated BV2 cells were stimulated with LPS (100 ng/ml, 24 h) and ATP (5 mM, 30 min). (a–c) Expression of NLRP3, pro-caspase-1, pro-IL-1β, full-length GSDMD and cleaved GSDMD N-terminal in cell lysate (Ly) was detected by an immunoblot assay (a). The relative expression levels were quantified (c). Actin was used as an internal loading control. The cleaved caspase-1 and cleaved IL-1β in the supernatant (SN) were also detected by an immunoblot assay (a) and quantified as normalized to the control group (b). (d) ELISA of IL-1β in supernatants from different-treated BV2 cells. (e–f) Treated BV2 cells were costained with YO-PRO-1 (green), a small (629.3 Da) membrane impermeable but pyroptosis-pole permeable dye, and Eth-D2 (red), a larger (1292.7 Da) membrane and pyroptosis-pole impermeable dye, to identify cells with discrete membrane pores. Hoechst staining (blue) indicates total cells. Treatment with 0.1% Triton was used as the positive control. Scale bar, 40 µm. (f) Quantitative analysis of cells that stained positive for YO-PRO-1 and negative for Eth-D2. A total of 15 fields/group (3 wells/group and 5 fields/well) cells were counted. Data are shown as the mean ± SEM of three to four independent experiments. *P < 0.05, **P < 0.01 and ***P < 0.001 by one-way ANOVA followed by Tukey's post hoc test. Ctl, untreated control; Qu, quercetin; LPS, lipopolysaccharide; Ly, lysate; SN, supernatant. (For interpretation of the references to colour in this figure legend, the reader is referred to the Web version of this article.)

3.6. Autophagy inhibition reverses the suppressive effect of Qu on mito-ROS accumulation, mitochondrial dysfunction and inflammatory factors expression

To further test whether mitophagy is one of the main mechanisms of the anti-inflammatory effect of Qu, the autophagy inhibitor, 3-MA, was used. We found that the protective effects of Qu on mitochondrial injury, including reduced mtROS acumulation (Fig. 6a and b), and alleviated mitochondrial dysfunction, as evidenced by fractured morphology and reduced number by immunostaining for Tomm20 (Fig. 6c and d), were significantly blocked by 3-MA. Furthermore, the inhibitory effect of Qu on LPS + ATP-induced NLRP3 inflammasome activation, including decreased pro-IL-1β protein (Fig. 6e) and reduced IL-1β maturation and

release (Fig. 6f and g) in BV2 cells, were significantly blocked by 3-MA. These results collectively indicate that Qu inhibits NLRP3 inflammasome activation through promoting mitophagy to alleviate mitochondrial ROS stress.

3.7. Quercetin suppresses microglia activation-mediated neurotoxicity in vitro

Activated microglia release inflammatory mediators that exert neurotoxic effects in many disorders [5,6]. We next investigated whether the inhibition of microglial activation by Qu protects neurons from inflammatory injury. To this end, primary mesencephalic TH+ dopaminergic neurons and hippocampal MAP+ neurons were cultured,
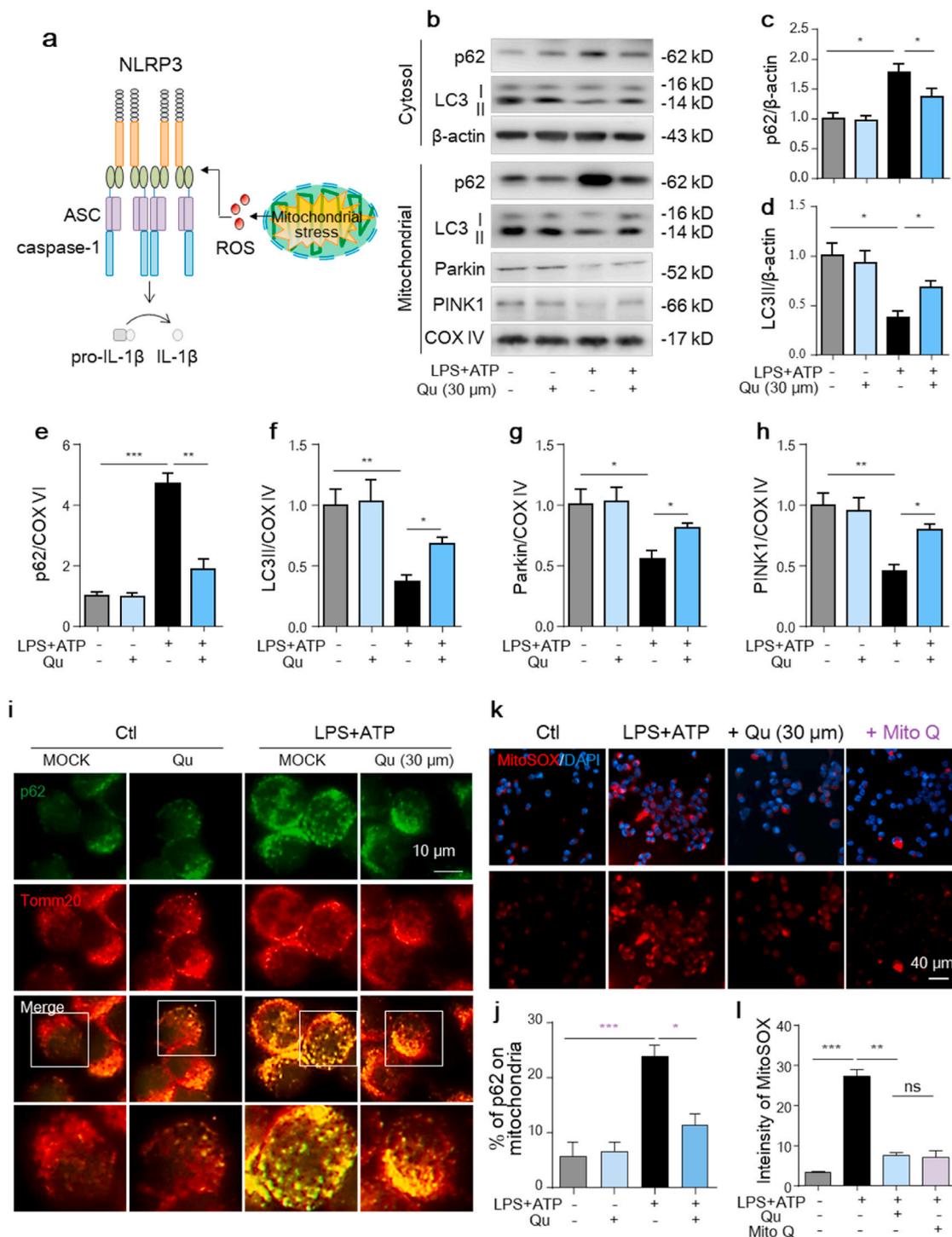
Fig. 5. Qu promotes mitophagy and decreases the mitochondrial ROS production in LPS + ATP-treated BV2 cells.

Qu (30 μm, 1 h) pretreated BV2 cells were stimulated with LPS (100 ng/ml, 24 h) and ATP (5 mM, 30 min).

(a) Increased damaged mitochondria functions as the second signal to promote NLRP3 inflammasome assembly and activation, which ultimately induces pyroptosis and IL-1β release.

(b–h) Representative immunoblots (b) and quantitative analysis of p62 and LC3II in the cytosol and mitochondrial protein extracts of BV2 cells. Quantified data are normalized to the control group.

(i–j) Representative images of the intracellular distribution of p62 and mitochondria (Tomm20) in BV2 cells as analyzed by confocal microscopy (i). Scale bar, 10 μm. The number of cells with p62 aggregation on mitochondria was quantified (j) (n = 12 fields/group; 3 wells/group and 4 fields/well).

BV2 cells were treated with Qu (30 μM, 1 h) or Mito Q (1 μM, 1 h) followed by LPS (100 ng/ml, 24 h) and ATP (5 mM, 30 min) stimulation.

(k–l) Mitochondrial ROS levels were assessed by staining with MitoSOX and analyzed using confocal microscopy (k). DAPI was used to stain nuclei (blue). Scale bar, 40 μm. Quantification of MitoSOX fluorescence intensity (l).

Data are shown as the mean ± SEM from three to five independent experiments. *$P < 0.05$, **$P < 0.01$ and ***$P < 0.001$ by one-way ANOVA followed by Tukey's post hoc test. Ctl, untreated control; Qu, quercetin; LPS, lipopolysaccharide; Mito Q: mitoquinone mesylate. . (For interpretation of the references to colour in this figure legend, the reader is referred to the Web version of this article.)
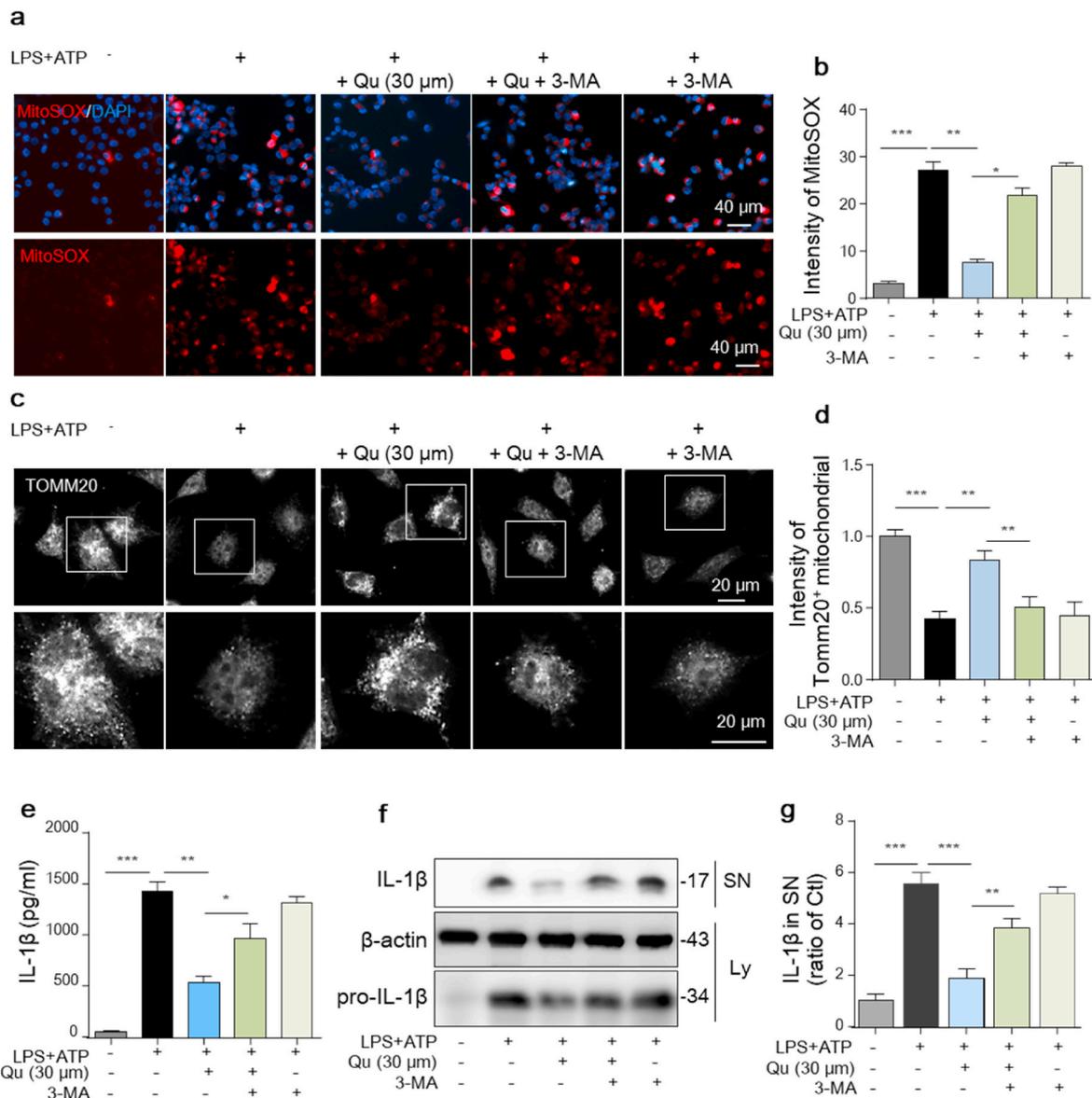
Fig. 6. Inhibiting autophagy reverses the protective effect of Qu on LPS + ATP-induced mitochondrial injury and inflammation in BV2 cells. BV2 cells were treated with 3-MA (5 mM, 1 h
) before Qu (30 μM, 1 h) treatment followed by LPS (100 ng/ml, 24 h) and ATP (5 mM, 30 min) stimulation.
(a–b) Mitochondrial ROS levels were assessed by staining with MitoSOX and analyzed using confocal microscopy (a). DAPI was used to stain nuclei (blue). Scale bars, 40 μm. Quantification of MitoSOX fluorescence intensity using ImageJ software (b).
(c–d) Mitochondrial morphology in BV2 cells were monitored and pictured by immunostaining for Tomm20. Scale bars, 20 μm.
(e) ELISA of IL-1β in supernatants from differently treated BV2 cells.
(f–g) Expression of pro-IL-1β in the cell lysate (Ly) and cleaved IL-1β in the supernatant (SN) were detected by an immunoblot assay (f) and quantified as normalized to the control group (g). Data are shown as the mean ± SEM from three to five independent experiments. *$P < 0.05$, **$P < 0.01$ and ***$P < 0.001$ by one-way ANOVA followed by Tukey's post hoc test. Ctl, untreated control; Qu, quercetin; LPS, lipopolysaccharide; 3-MA, 3-methyladenine. . (For interpretation of the references to colour in this figure legend, the reader is referred to the Web version of this article.)

and microglial-derived conditioned medium (MCM) was added (Fig. 7a). As shown in Fig. 7b, the addition of conditioned medium from LPS + ATP-stimulated microglia led to the reduced viability of cultured mesencephalic and hippocampal neurons, and Qu significantly attenuated neuron damage (Fig. 7b). This protection of Qu was blunted by adding pro-inflammatory factor IL-1β to cultured neurons (Fig. 7b). By immune-staining assay, we found that the TH[+] neural processes and neurites of dopaminergic neurons were significantly shorted when cultured with LPS+ATP-treated microglia medium, evidenced by ICH morphological analysis (Fig. 7c and d). However, this neurotoxicity was reduced by adding conditioned medium from Qu-pretreated microglia,

and the protection of Qu was blunted by adding IL-1β to the neuronal culture (Fig. 7c and d). Consistent with the CCK-8 assay in Fig. 7b, under fluorescence microscope, we found that the hippocampal neurons showed high-density fluorescence with nuclear shrinkage and chromatic agglutination when treated with LPS + ATP-stimulated microglia-conditioned medium, evidenced by the Hoechst staining assay (Fig. 7e and f). Pretreatment of microglia with Qu alleviated LPS + ATP-induced karyopyknosis and chromatin condensation, which was reversed by IL-1β administration (Fig. 7e and f). These data demonstrate that the anti-inflammatory effect of Qu exerts a neuroprotective effect in cultured primary neurons.
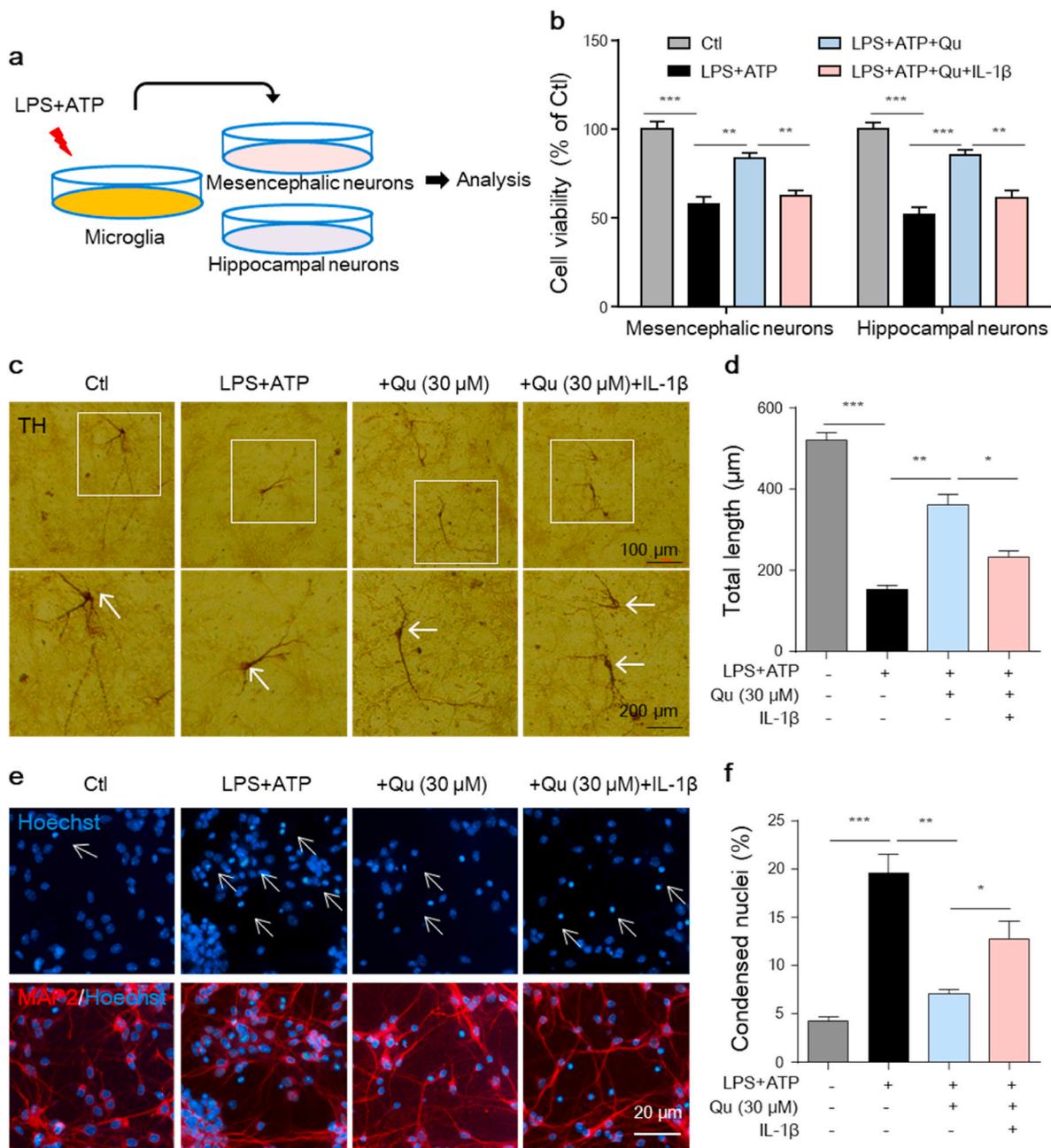
Fig. 7. Qu protects against microglia activation-mediated neurotoxicity *in vitro*.
Mesencephalic and hippocampal primary neurons were treated with conditioned media (CM) from miroglia
cells exposed to LPS
+
ATP with or without Qu (30 μM) pretreatment or treated with CM from LPS + ATP + Qu treated-microglia plus recombinant IL-1β (50 ng/ml) for 24 h
(a) Protocol of treatment. Primary mesencephalic and hippocampal neurons were incubated with the microglia-derived CM mixed with neurobasal medium for 12 h followed by the bioassay.
(b) Cell viability of primary neurons was assayed by the CCK8 assay.
(c–d) Representative images of TH immunostaining of mesencephalic neurons (c). White arrows indicate the nucleus. Scale bars as indicated. Quantification of the total neurite length (d). There was a total of 27–30 neurons/condition (3 wells/group and 9–10 neurons/well).
(e–f) Primary hippocampal neurons were stained with Hoechst and imaged by fluorescence microscopy (e).Quantitative analysis of the Hoechst positive cells with condensed nuclei (f). Scale bar, 20 μm.
Data are shown as the mean ± SEM of three independent experiments. *$P < 0.05$, **$P < 0.01$ and ***$P < 0.001$ by one-way ANOVA followed by Tukey's post hoc test. Ctl, untreated control; Qu, quercetin; LPS, lipopolysaccharide.

3.8. Qu suppresses microglia-mediated neurotoxicity in a mouse depression model

To study the anti-inflammatory and neuroprotective role of Qu *in vivo*, we first constructed the accepted inflammatory-related depression model as reported [5,6]. C57BL/6 mice were injected with LPS for 5 days to induce depression. Mice were administered different doses of Qu (30 and 60 mg/kg b.w.) 3 days prior to and during the duration of LPS modeling followed by behavioral tests (Fig. 8a).

As inflammasome-regulated IL-1β is an essential mediator involved
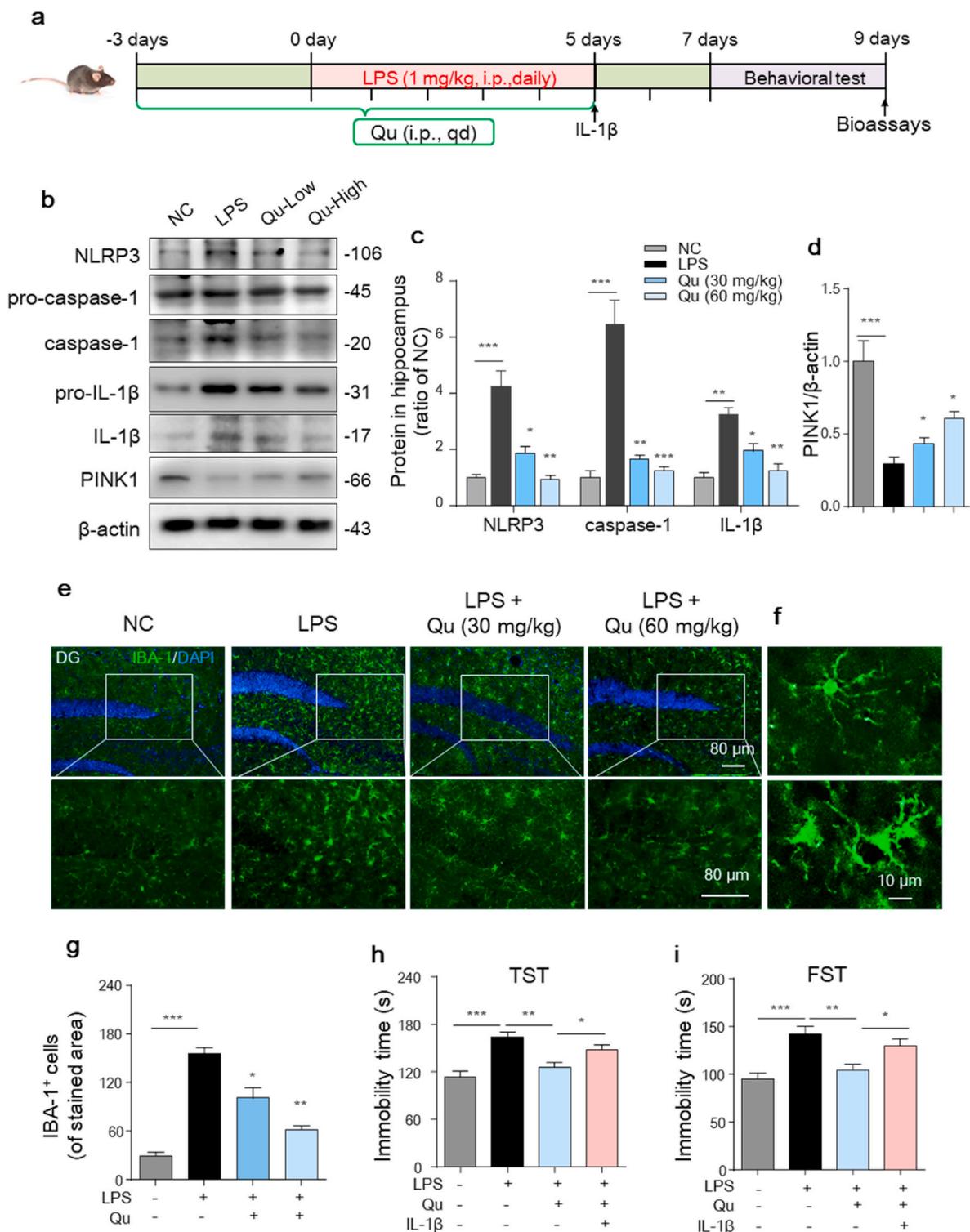
Fig. 8. Qu inhibits LPS-induced glial proliferation and NLRP3 inflammasome activation in the hippocampus of a depression mouse model.

(a) Timeline of the experimental procedure in the LPS-induced depression mouse model.

(b–d) Protein levels of NLRP3, caspase-1, pro-IL-1β, IL-1β and PINK1 in mouse hippocampal homogenates were analyzed by western blot (b) and quantified (c–d). n = 4–6 mice/group.

(e–g) Immunofluorescent staining of IBA-1-positive microglia in hippocampal sections (e) with quantification (g). Scale bars, 80 μm n = 4–6 mice/group. (f) Upper and lower magnified images represent resting and activated microglia, respectively. Scale bar, 10 μm.

(h–i) The tail suspension test (TST) (h) and forced swim test (FST) (i) of the indicated mouse. (n = 8–10 mice/group).

Values are shown as the mean ± SEM. *P < 0.05, **P < 0.01 and ***P < 0.001 by one-way ANOVA followed by Tukey's post hoc test. NC, negative control; Qu, quercetin; LPS, lipopolysaccharide. . (For interpretation of the references to colour in this figure legend, the reader is referred to the Web version of this article.)

in the development of depression [44], we first investigated the activation of the NLRP3 inflammasome in the hippocampus. As shown in Fig. 8b and c, the LPS mice developed markedly increased expression of NLRP3 as well as active caspase-1 and matured IL-1β levels compared with control mice. Qu treatment significantly inhibited NLRP3/caspase-1/IL-1β axis activation in a dose-dependent manner (Fig. 8b and c). We also found that Qu treatment alleviated the reduction of PINK1 in the hippocampus of LPS-treated mice (Fig. 8b, d). Furthermore, immunofluorescence staining of IBA-1 indicated the activation of microglia as evidenced by increased cell density and activated amoeba-like morphology (Fig. 8f) in both the hippocampus (Fig. 8e–g) and cortex (Fig. S 2a-b) of the LPS mice. The activation was further confirmed by significantly increased CD68 fluorescence intensity in IBA-1$^+$ cells in the hippocampus of LPS mice (Fig. S 2c-d). Qu treatment significantly suppressed the microglia activation (Fig. 8e, g and Fig. S 2a-d). Then, to evaluate the effect of Qu on depressant activity, behavioral tests were employed. As shown in Fig. 8 h-i, the immobility time was significantly higher in LPS-treated mice than in control mice in both the TST (Fig. 8h) and FST (Fig. 8i), which was ameliorated in the Qu-treated group.

As IL-1β is the final effector of NLRP3 inflammation, studies have demonstrated that administration of IL-1β mimics the effects of induced depression [45] and blocks the antidepressant effect of caspase-1 deletion in mice [46]. Thus, we investigated whether administration of IL-1β blocks the antidepressant effect of Qu. As shown in Fig. 8h and i, IL-1β administration significantly blunted the neuroprotective effects of Qu as evidenced by reversed alleviation of immobility performance in the TST and FST. These results collectively suggest that inhibition of NLRP3/caspase-1/IL-1β activation accounts for the antidepressant effect of Qu in the LPS-induced depression model.

3.9. Qu suppresses microglia-mediated neurotoxicity and alleviates the loss of DA neurons in the SNpc of a PD mouse model

Both enhanced neuroinflammation and weakened mitophagy are involved in the pathogenesis of Parkinson's disease [47]. To evaluate the neuroprotective role of Qu in PD, we conducted a LPS-induced PD mouse model as our previously reported [9]. Briefly, C57BL/6 mice were stereotactically microinjected with LPS in the SNpc and received Qu treatment (30 and 60 mg/kg b.w.) 3 days prior to and 7 days afterwards the LPS injection (Fig. 9a). After model induction, the activation of NLRP3 inflammation in the midbrain was observed. The protein levels of NLRP3, active caspase-1 and IL-1β were markedly increased in the midbrain in LPS-treated mice, which was prevented by Qu (Fig. 9b and c). IHF staining also confirmed increased IBA-1$^+$ microglial density in the SNpc of LPS-microinjected mice, which was attenuated by Qu pre-treatment (Fig. 9f and g). Regarding neuroprotection, the TH protein levels and TH$^+$ neuron numbers in the mouse SNpc were detected by western blot and immunostaining. The LPS challenge resulted in a significant reduction in TH protein expression (Fig. 9d and e) and TH$^+$ neuron numbers (Fig. 9h and i), which was alleviated by Qu treatment. We also examined the performance of the Qu-treated mice in behavioral coordination. The data obtained for the rotarod test demonstrated that Qu improved the LPS-inhibited movement performance in mice (Fig. 9j).

Furthermore, administration of IL-1β post Qu treatment significantly blunted the neuroprotective effects of Qu as evidenced by increased reduction of TH protein (Fig. 9d and e) and loss of TH$^+$ neurons (Fig. 9h and i) in the SNpc of mouse and worsened motor performance in the retarod test (Fig. 9j). This evidence confirms that Qu exerts neuroprotective effects in both depression and PD mice by inhibiting microglial activation.

4. Discussion

The present study showed that the natural bioflavonoid compound Qu is a key inhibitor of microglial activation by orchestrating both the first and second signals of the NLRP3 inflammasome. First, Qu inhibited the LPS-induced increase in the activity of NF-κB signal and the expression of NLRP3 inflammasome-related proteins. Second, Qu acted as a key link by which mitophagic signaling could inhibit mtROS-amplified NLRP3 inflammasome assembly and final activation. Our results demonstrated that the mitophagy pathway is a key regulatory loop through which Qu promotes damaged mitochondrial clearance to reduce mtROS accumulation and subsequent NLRP3 inflammasome assembly. Collectively, we focused on both transcription and mitophagy-regulated mtROS inhibition signals to alleviate inflammation in microglial cells to clarify the neuroprotective effect of Qu by preventing neuronal degeneration due to excessive inflammatory toxicity (Fig. 10).

Recent studies have revealed that direct, intracellular neurotoxins, such as impaired mitochondrial respiration, increased ROS and decreased ATP production in neurons cannot completely clarify the mechanisms of many brain disorders, including depression and NDDs. Structurally, neurons are surrounded by a large number of glial cells [2]. Functionally, the glial cell-mediated microenvironment surrounding neurons plays an important role in neuronal homeostasis and activity maintenance [1,3,48]. Multiple studies have proposed that sterile inflammation has a crucial role in neuronal damage and is implicated in the pathophysiology of many CNS injuries [8,49]. Microglia are the dominant inflammatory cells among all glial cells [50], which act as the first defense of the CNS and initiate inflammatory signaling to secrete damage-associated molecules into the extracellular milieu in case of danger [51]. However, uncontrolled excessive or persistent activation of microglia and its mediated inflammation are quite harmful and are involved in diverse CNS diseases, including PD, AD and depression [4, 41]; thus, the activation of microglia should be tightly controlled. We previously reported increased activation of the NLRP3 inflammasome in microglia in the SNpc of both MPTP- and LPS-injected mice, which aggravates the death of dopaminergic (DA) neurons [9], and we also reported that targeted inhibition of microglial activation alleviates DA neuron loss [9]. All the above findings demonstrate that excessively activated microglia are toxic to neurons and that targeting microglial activation inhibition represents an important potential strategy for treating various neuronal disorders.

Interestingly, in the present study, we demonstrated that Qu, a natural flavonoid component, strongly suppressed not only the proinflammatory factor production but also the phagocytosis activity in LPS-treated microglial cells. Moreover, our results demonstrated that Qu was a natural inhibitor of NLRP3 inflammasome activation in microglia, which alleviated the release of proinflammatory factor IL-1β. The inflammasome, as a crucial component of innate immune responses and inflammation, is a family of cytosolic multimeric protein complexes that are sensors of DAMPs [18,19]. Although several inflammasomes have been described, the NLRP3 inflammasome is highly expressed in microglia and especially relevant to neurotoxicity, which is extensively involved in many brain diseases [8]. Two signaling pathways, both primary transcriptional activators and second assembly activators, are required for NLRP3 inflammasome activation [19]. By measuring the level of secreted IL-1β in the supernatant of cultured BV2 cells, we first found that Qu reduced the levels of IL-1β protein in LPS-treated BV2 cells, which conforming the inhibitory effect of Qu on inflammasome activation. Then, we found that Qu inhibited the LPS-induced upregulation of NLRP3 inflammasome-related proteins, including NLRP3, pro-caspase-1 and pro-IL-1β, in BV2 cells. The above results confirmed the inhibitory effect of Qu on at least the first signal of the NLRP3 inflammasome.

However, the cleavage of pro-IL-1β into mature IL-1β requires the assembly step of the NLRP3/ASC/pro-caspase-1 complex. When NLRP3 binds to ASC, it recruits and induces pro-caspase-1 cleavage into active caspase-1, which then cleaves pro-IL-1β to produce mature IL-1β [19]. In addition to the first priming step, many regulatory mechanisms have been studied focusing on the attenuation of the assembly step of NLRP3 inflammasome signaling. Among them, the induction of autophagy has
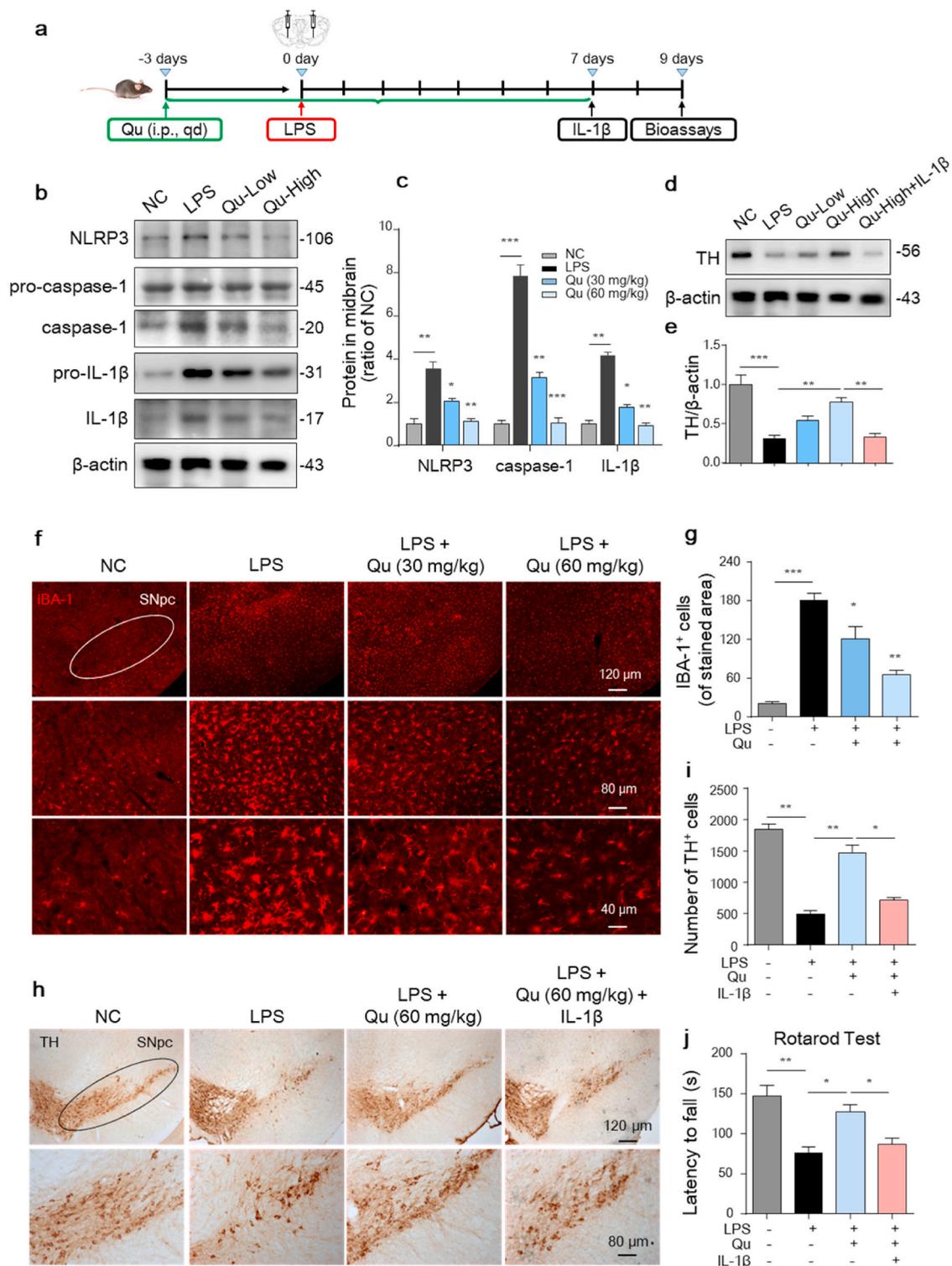
Fig. 9. Inhibitory effect of Qu on NLRP3 inflammasome activation-related neurotoxicity in LPS-induced PD mice.

(a) Timeline of the experimental procedure in the LPS-induced mouse PD model.

(b–c) Protein levels of NLRP3, caspase-1, pro-IL-1β and IL-1β in mouse mesencephalic homogenates were analyzed by western blot (b) and quantified (c). Low indicated 30 mg/kg b.w., high indicated 60 mg/kg b.w. dose.

(d–e) Expression of TH protein levels in mesencephalon from the indicated mice was analyzed by immunoblotting (d) and quantitative analyzed (e).

(f–g) Immunofluorescent staining of IBA-1-positive microglia in SNpc sections (f) and quantitative analyzed (g). Scale bars as indicated.

(h–i) Immunohistochemical images of TH-positive DA neurons in SNpc sections (h) with quantification (i). Scale bars as indicated.

(j) Rotarod test in different groups at the end of the experiment. (n =

7–

9 mice/group).

Values are shown as the mean ± SEM of three independent experiments. *$P < 0.05$, **$P < 0.01$ and ***$P < 0.001$ by one-way ANOVA followed by Tukey's post hoc test. n = 4–6 mice per group in (b–i). NC, negative control; Qu, quercetin; LPS, lipopolysaccharide; SNpc, substantia nigra pars compacta.
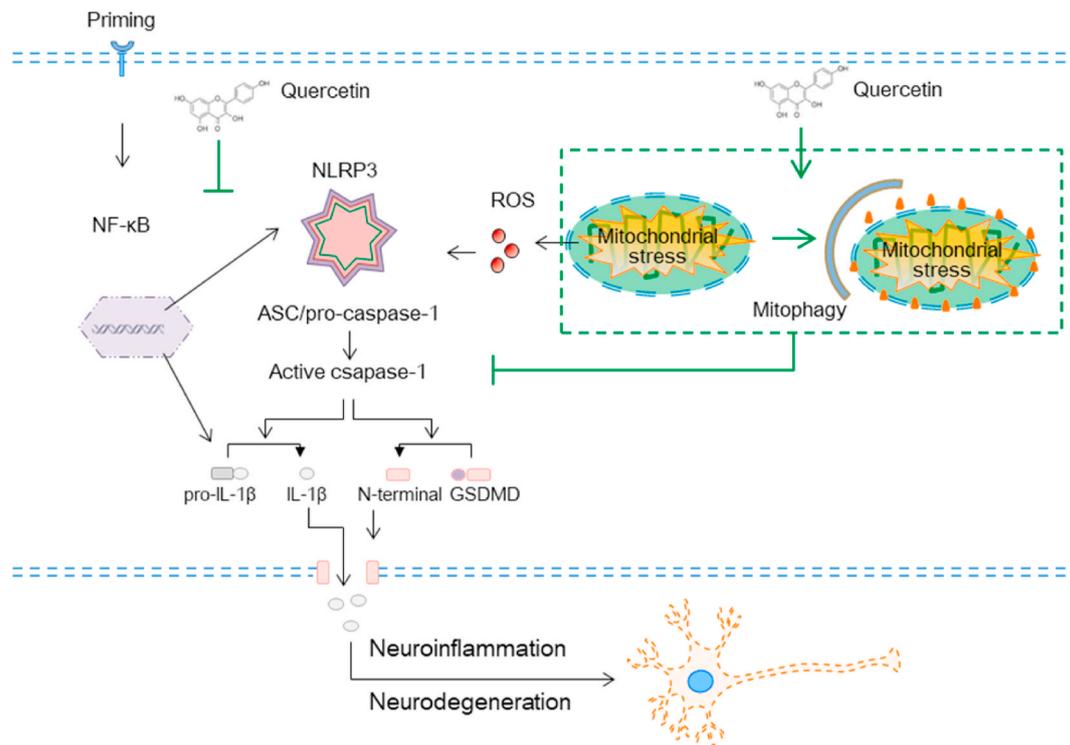
Fig. 10. Proposed model depicting Qu as a mitophagy promoter to degrade damaged mitochondria and prevent mtROS accumulation, which alleviates NLRP3 inflammation assembly and resulted IL-1β release from microglia, consequently, suppressing the neurotoxicity process in depression and Parkinson's disease.

been reported to negatively regulate NLRP3 inflammasome activation, which mediates the clearance of harmful substrates or secondary signals, such as damaged mitochondria in cells [24,25]. Recent studies have shown that mitophagy-dependent degradation of damaged mitochondria alleviates NLRP3 activation [11,20] but the mechanism is not fully defined. Damaged mitochondria are thought to release or display signals, such as mtROS and mtDNA, which function as assembly activators to promote and amplify NLRP3 inflammasome activation [19]. Based on the above facts, we reasoned that promoting elimination of damaged mitochondria may attenuate NLRP3 assembly. Interestingly, we found that Qu promoted mitophagy, which enhanced the mitophagic clearance of damaged mitochondria and reduced the accumulation of mtROS in LPS-treated BV2 cells. Furthermore, specific inhibition of mitophagy by 3-MA blunted the inhibitory effect of Qu on IL-1β maturation and release from LPS and ATP-treated BV2 cells, suggesting that Qu inhibits the second assembly signal of the NLRP3 inflammasome in microglial cells in a mitophagy-dependent manner.

Another remarkable finding of the present study is that we determined that Qu had a robust effect against pyroptosis in LPS + ATP-treated BV2 cells as evidenced by both Western blot and dye uptake assays. Pyroptosis is an inflammatory type of programmed cell death that is required for IL-1β secretion [13]. Activation of the NLRP3 inflammasome results in the cleavage of full-length GSDMD protein to generate the GSDMD N-terminus, which then forms large oligomeric pores in the plasma membrane, allowing for the release of mature IL-1β. First, we found that the protein level of the GSDMD N-terminus was increased in BV2 cells stimulated with LPS plus ATP, and this effect was alleviated by Qu pretreatment. In addition to GSDMD cleavage, pore formation on the plasma membrane is another functional characterization of pyroptosis, which allows only molecules with a diameter less than 10–13 nm to pass through. Thus, small (YO-PRO-1 iodide, 629 Da) pore permeable and large (Eth-D2, 1,293 Da) pore impermeable dyes were combined to visualize pyroptotic cells by fluorescence microscopy [14]. This dye uptake assay showed that pretreatment with Qu significantly decreased the LPS + ATP-induced formation of discrete pores in

the plasma membrane of BV2 cells, thus confirming the pyroptosis-inhibiting effect of Qu on the microglial activation process.

These findings implied that Qu might be a promising natural compound for the inhibition of microglial activation and therapy of neuroinflammation-related neuronal injury. For clarification, we conducted primary neuron cultures, which were further coincubated with conditioned medium from LPS + ATP (or Qu pretreatment)-stimulated microglia. In cultured microglia, we found that Qu inhibited LPS + ATP-induced NLRP3 inflammasome activation, the related pyroptosis and consequently IL-1β release. Furthermore, Qu alleviated subsequent dendritic injury and cell apoptosis induced by activated microglia-derived conditioned medium in both cultured primary mesencephalic and hippocampal neurons. We also found that the further administration of recombinant IL-1β in neuronal culture reversed the role of Qu in preventing microglial activation-induced toxicity in primary neurons, indicating that Qu exerts a neuroprotective effect through microglial NLRP3/IL-1β pathways *in vitro*. In addition, we provided evidence that Qu pretreatment ameliorated LPS-induced depression behaviors and dopaminergic neuron loss in depression and PD mouse models, respectively, by inhibiting microglial activation in the NLRP3/IL-1β dependent pathway.

Quercetin is a natural flavonoid that is ubiquitously present in diet and many traditional medicinal herbs, which are valuable sources for lead compounds identification and their subsequent drugs discovery. Studies indicated that supplementation with quercetin-enriched foods or supplements can increase quercetin concentrations in plasma easy, exerting beneficial effects in the prevention and treatment of a variety of diseases including NDDs [27]. However, many neurodegenerative changes are irreversible in the later stages. And study indicated that quercetin showed only a modest protective effect when administered after the diagnosis in a severe model of PD [52]. Thus, developing a safe and effective strategy and starting the intervention at an early age may yield greater neuroprotection. To this point, our *in vivo* treatment paradigm, in which we administered quercetin prior to the models induction (LPS challenge), mimics the preventive approach. And, our

results support the concept that quercetin can be orientated on the prevention rather than just on therapy to get an earlier benefit.

In conclusion, the results in this study provided strong evidence for the preventive/therapeutic activity of Qu against microglial inflammatory activation and its mediated neurotoxicity *in vitro* and *in vivo*. The mechanisms underlying the activity of Qu involved both inhibition in the transcription stage and mitophagy-mediated mtROS elimination-dependent NLRP3 inflammasome inactivation in the assembly stage, thus resulting in reduced NLRP3-/pyroptosis-mediated IL1β release from microglia. The data presented here are consistent with the concept that microglia may be an important target for treating various brain injuries and might help guide decisions regarding the use of natural molecular Qu as an anti-inflammatory agent in microglial activation and related neuroinflammatory conditions.

CRediT authorship contribution statement

Xiaojuan Han: designed and performed most of the experiments, Formal analysis, and wrote the manuscript. **Tianshu Xu:** and, performed experiments and analyzed the data. **Qijun Fang:** and, performed experiments and analyzed the data. **Huajun Zhang:** and, performed experiments and analyzed the data. **Lijun Yue:** performed experiments and analyzed the data, performed experiments and analyzed the data. **Gang Hu:** helped in designing the experiments. **Lingyun Sun:** conceived the study concept and designed the experiments.

Declaration of competing interest

The authors declare no competing interests.

Acknowledgments and Funding

Appendix A. Supplementary data

Supplementary data to this article can be found online at https://doi.org/10.1016/j.redox.2021.102010.

References

[1] N.J. Allen, B.A. Barres, Neuroscience: glia - more than just brain glue[J], Nature 457 (7230) (2009) 675–677.

[2] R. von Bernhardi, B.J. Eugenin-von, B. Flores, et al., Glial cells and integrity of the nervous system[J], Adv. Exp. Med. Biol. 949 (2016) 1–24.

[3] Q. Li, B.A. Barres, Microglia and macrophages in brain homeostasis and disease[J], Nat. Rev. Immunol. 18 (4) (2018) 225–242.

[4] M. Colonna, O. Butovsky, Microglia function in the central nervous system during Health and neurodegeneration[J], Annu. Rev. Immunol. 35 (1) (2017) 441–468.

[5] S.A. Wolf, H.W.G.M. Boddeke, H. Kettenmann, Microglia in physiology and disease [J], Annu. Rev. Physiol. 79 (1) (2017) 619–643.

[6] W.M. Song, M. Colonna, The identity and function of microglia in neurodegeneration[J], Nat. Immunol. 19 (10) (2018) 1048–1058.

[7] P. Rider, Y. Carmi, I. Cohen, et al., Biologics for targeting inflammatory cytokines, clinical uses, and limitations[J], Int. J. Cell Biol. 2016 (2016) 9259611–9259646.

[8] S. Voet, S. Srinivasan, M. Lamkanfi, et al., Inflammasomes in neuroinflammatory and neurodegenerative diseases[J], EMBO Mol. Med. 11 (6) (2019) (n/a-n/a).

[9] X. Han, S. Sun, Y. Sun, et al., Small molecule-driven NLRP3 inflammation inhibition via interplay between ubiquitination and autophagy: implications for Parkinson disease[J], Autophagy 15 (11) (2019) 1860–1881.

[10] M. Lamkanfi, V.M. Dixit, Mechanisms and functions of inflammasomes[J], Cell 157 (5) (2014) 1013–1022.

[11] J.P. de Rivero Vaccari, W.D. Dietrich, R.W. Keane, Activation and regulation of cellular inflammasomes: gaps in our knowledge for central nervous system injury [J], J. Cerebr. Blood Flow Metabol. 34 (3) (2014) 369–375.

[12] M.T. Heneka, R.M. McManus, E. Latz, Inflammasome signalling in brain function and neurodegenerative disease[J], Nat. Rev. Neurosci. 19 (10) (2018) 610–621.

[13] J. Shi, W. Gao, F. Shao, Pyroptosis: gasdermin-mediated programmed necrotic cell death[J], Trends Biochem. Sci. 42 (4) (2017) 245–254.

[14] S.E. Adamczak, J.P. de Rivero Vaccari, G. Dale, et al., Pyroptotic neuronal cell death mediated by the AIM2 inflammasome[J], J. Cerebr. Blood Flow Metabol. 34 (4) (2014) 621–629.

[15] Z. He, S. An, J. Chen, et al., Neural progenitor cell pyroptosis contributes to Zika virus-induced brain atrophy and represents a therapeutic target[J], Proc. Natl. Acad. Sci. U. S. A. 117 (38) (2020) 23869–23878.

[16] R.A. Aglietti, E.C. Dueber, Recent insights into the molecular mechanisms underlying pyroptosis and gasdermin family functions[J], Trends Immunol. 38 (4) (2017) 261–271.

[17] M. Aziz, A. Jacob, P. Wang, Revisiting caspases in sepsis[J], Cell Death Dis. 5 (11) (2014) e1526.

[18] Y. He, H. Hara, G. Nunez, Mechanism and regulation of NLRP3 inflammasome activation[J], Trends Biochem. Sci. 41 (12) (2016) 1012–1021.

[19] E.I. Elliott, F.S. Sutterwala, Initiation and perpetuation of NLRP3 inflammasome activation and assembly[J], Immunol. Rev. 265 (1) (2015) 35–52.

[20] Z. Zhong, A. Umemura, E. Sanchez-Lopez, et al., NF-kappaB restricts inflammasome activation via elimination of damaged mitochondria[J], Cell 164 (5) (2016) 896–910.

[21] K. Nakahira, J.A. Haspel, V.A.K. Rathinam, et al., Autophagy proteins regulate innate immune responses by inhibiting the release of mitochondrial DNA mediated by the NALP3 inflammasome[J], Nat. Immunol. 12 (3) (2011) 222–230.

[22] J. Yu, H. Nagasu, T. Murakami, et al., Inflammasome activation leads to Caspase-1-dependent mitochondrial damage and block of mitophagy[J], Proc. Natl. Acad. Sci. - PNAS 111 (43) (2014) 15514–15519.

[23] R. Zhou, A.S. Yazdi, P. Menu, et al., A role for mitochondria in NLRP3 inflammasome activation[J], Nature 469 (7329) (2011) 221–225.

[24] T. Saitoh, N. Fujita, M.H. Jang, et al., Loss of the autophagy protein Atg16L1 enhances endotoxin-induced IL-1β production[J], Nature 456 (7219) (2008) 264–268.

[25] K. Nakahira, J.A. Haspel, V.A.K. Rathinam, et al., Autophagy proteins regulate innate immune responses by inhibiting the release of mitochondrial DNA mediated by the NALP3 inflammasome[J], Nat. Immunol. 12 (3) (2011) 222–230.

[26] R.J. Youle, D.P. Narendra, Mechanisms of mitophagy[J], Nat. Rev. Mol. Cell Biol. 12 (1) (2011) 9–14.

[27] M. Russo, C. Spagnuolo, I. Tedesco, et al., The flavonoid quercetin in disease prevention and therapy: facts and fancies[J], Biochem. Pharmacol. 83 (1) (2012) 6–15.

[28] A.W. Boots, G.R.M.M. Haenen, A. Bast, Health effects of quercetin: from antioxidant to nutraceutical[J], Eur. J. Pharmacol. 585 (2–3) (2008) 325–337.

[29] D.R. Ferry, A. Smith, J. Malkhandi, et al., Phase I clinical trial of the flavonoid quercetin: pharmacokinetics and evidence for in vivo tyrosine kinase inhibition[J], Clin. Canc. Res. 2 (4) (1996) 659–668.

[30] K. Wang, R. Liu, J. Li, et al., Quercetin induces protective autophagy in gastric cancer cells: involvement of Akt-mTOR- and hypoxia-induced factor 1α-mediated signaling[J], Autophagy 7 (9) (2014) 966–978.

[31] X. Han, J. Zhu, X. Zhang, et al., Plin4-Dependent lipid droplets Hamper neuronal mitophagy in the MPTP/p-Induced mouse model of Parkinson's disease[J], Front. Neurosci. 12 (2018) 397.

[32] A. Shah, L. Xia, H. Goldberg, et al., Thioredoxin-interacting protein mediates high glucose-induced reactive oxygen species generation by mitochondria and the NADPH oxidase, Nox4, in mesangial cells[J], J. Biol. Chem. 288 (10) (2013) 6835–6848.

[33] C. Qiao, L. Zhang, X. Sun, et al., Caspase-1 deficiency alleviates dopaminergic neuronal death via inhibiting caspase-7/AIF pathway in MPTP/p mouse model of Parkinson's disease[J], Mol. Neurobiol. 54 (6) (2017) 4292–4302.

[34] Z.M. Shu, X.D. Shu, H.Q. Li, et al., Ginkgolide B protects against ischemic stroke via modulating microglia polarization in mice[J], CNS Neurosci. Ther. 22 (9) (2016) 729–739.

[35] Y. Zhang, L. Du, Y. Bai, et al., CircDYM ameliorates depressive-like behavior by targeting miR-9 to regulate microglial activation via HSP90 ubiquitination[J], Mol. Psychiatr. 25 (6) (2020) 1175–1190.

[36] T. Hu, X.Y. Lu, J.J. Shi, et al., Quercetin protects against diabetic encephalopathy via SIRT1/NLRP3 pathway in db/db mice[J], J. Cell Mol. Med. 24 (6) (2020) 3449–3459.

[37] M. Harwood, B. Danielewska-Nikiel, J.F. Borzelleca, et al., A critical review of the data related to the safety of quercetin and lack of evidence of in vivo toxicity, including lack of genotoxic/carcinogenic properties[J], Food Chem. Toxicol. 45 (11) (2007) 2179–2205.

[38] D.W. Lamson, M.S. Brignall, Antioxidants and cancer, part 3: quercetin[J], Alternative Med. Rev. 5 (3) (2000) 196.

[39] X. Han, S. Zhao, H. Song, et al., Kaempferol alleviates LD-mitochondrial damage by promoting autophagy: implications in Parkinson's disease[J], Redox Biol. 41 (2021) 101911.

[40] H. Lui, J. Zhang, S.R. Makinson, et al., Progranulin deficiency promotes circuit-specific synaptic pruning by microglia via complement activation[J], Cell 165 (4) (2016) 921–935.

[41] H. Liu, Y. Han, T. Wang, et al., Targeting microglia for therapy of Parkinson's disease by using biomimetic ultrasmall nanoparticles[J], J. Am. Chem. Soc. 142 (52) (2020) 21730–21742.

[42] J. Ding, K. Wang, W. Liu, et al., Pore-forming activity and structural autoinhibition of the gasdermin family[J], Nature 535 (7610) (2016) 111–116.

[43] M. Lazarou, D.A. Sliter, L.A. Kane, et al., The ubiquitin kinase PINK1 recruits autophagy receptors to induce mitophagy[J], Nature 524 (7565) (2015) 309–314.

[44] M. Maes, C. Song, R. Yirmiya, Targeting IL-1 in depression[J], Expert Opin. Ther. Targets 16 (11) (2012) 1097–1112.

[45] I. Goshen, T. Kreisel, O. Ben-Menachem-Zidon, et al., Brain interleukin-1 mediates chronic stress-induced depression in mice via adrenocortical activation and hippocampal neurogenesis suppression[J], Mol. Psychiatr. 13 (7) (2008) 717–728.

[46] M. Li, H. Zheng, Y. Luo, et al., Gene deficiency and pharmacological inhibition of caspase-1 confers resilience to chronic social defeat stress via regulating the stability of surface AMPARs[J], Mol. Psychiatr. 23 (3) (2017) 556–568.

[47] W. Poewe, K. Seppi, C.M. Tanner, et al., Parkinson disease[J], Nat. Rev. Dis. Primers 3 (2017) 17013.

[48] S.A. Liddelow, K.A. Guttenplan, L.E. Clarke, et al., Neurotoxic reactive astrocytes are induced by activated microglia[J], Nature 541 (7638) (2017) 481–487.

[49] M.T. Heneka, M.P. Kummer, E. Latz, Innate immune activation in neurodegenerative disease[J], Nat. Rev. Immunol. 14 (7) (2014) 463–477.

[50] L.I. Labzin, M.T. Heneka, E. Latz, Innate immunity and neurodegeneration[J], Annu. Rev. Med. 69 (2018) 437–449.

[51] N. Lenart, D. Brough, A. Denes, Inflammasomes link vascular disease with neuroinflammation and brain disorders[J], J. Cerebr. Blood Flow Metabol. 36 (10) (2016) 1668–1685.

[52] M. Ay, J. Luo, M. Langley, et al., Molecular mechanisms underlying protective effects of quercetin against mitochondrial dysfunction and progressive dopaminergic neurodegeneration in cell culture and MitoPark transgenic mouse models of Parkinson's Disease[J], J. Neurochem. 141 (5) (2017) 766–782.